Synthetic communities of maize root bacteria interact and redirect benzoxazinoid metabolization

Lisa Thoenen[1,2], Tobias Zuest[1,3], Christine Pestalozzi[2], Marco Kreuzer[4], Pierre Mateo[1], Gabriel Deslandes[1], Christelle A.M. Robert[1], Rémy Bruggmann[4], Matthias Erb[1], Klaus Schlaeppi[1,2 #]

[1] Institute of Plant Sciences, University of Bern, Bern, Switzerland

[2] Department of Environmental Sciences, University of Basel, Basel, Switzerland

[3] Department of Systematic and Evolutionary Botany, University of Zurich, Zurich, Switzerland

[4] Interfaculty Bioinformatics Unit, University of Bern, Bern, Switzerland

Address correspondence to Klaus Schlaeppi, klaus.schlaeppi@unibas.ch

Running Head: "Benzoxazinoid metabolization by synthetic communities" (49 ch.)

Word count abstract: 182

Word count text: 5002

Author contributions

L.T. and K.S. designed the research; L.T. performed experiments. M.K. processed microbiome data, P.M. and T.Z. developed and performed metabolomic analyses. C.P. supported the writing of the manuscript. G.D. prepared the library for microbiome sequencing. C.A.M.R developed and validated the methods for metabolomic analysis. M.E. provided technical infrastructure and R.B. provided new analytic tools. L.T. and M.K. analysed the data and L.T. and K.S. wrote the manuscript. All authors revised the paper.

Abstract

Plant roots are colonised by diverse microbial communities. These communities are shaped by root exudates including plant specialized metabolites. Benzoxazinoids are such secreted compounds of maize. Individual microbes differ in their ability to tolerate and metabolize antimicrobial benzoxazinoids. To investigate how these traits combine in a community, we designed two synthetic communities of maize root bacteria that share six common strains and differ in their ability to metabolize benzoxazinoids based on the seventh strain. We exposed both communities to the benzoxazinoid MBOA (6-methoxybenzoxazolin-2(3H)-one) and found that the metabolizing community did not degrade MBOA to its aminophenoxazinone, as observed for individual strains, but as a community they formed the corresponding acetamide. MBOA shaped differential compositions of both communities and increased the fraction of MBOA-tolerant strains. The benzoxazinoid metabolizing community showed a higher tolerance to MBOA and was able to utilize MBOA as their sole carbon source for growth. Hence, bacterial interaction results in alternative benzoxazinoid metabolization and increases community performance in presence of these antimicrobial compounds. Future work is needed to uncover the genetics of this metabolic interaction and ecological consequences for the bacterial community and the host plant.

Importance

We investigated how maize root bacteria - alone or in community - tolerate and metabolize antimicrobial compounds of their host plant. We found the capacity to metabolize such a compound to impact bacterial community size and structure and most importantly, to benefit community fitness. We also found that interacting bacteria redirected the metabolisation of the antimicrobial compound to an alternative degradation product. Our work highlights the need to study the team work of microbes to uncover their community traits to ultimately understand the ecological consequences for the bacterial community and eventually the host plant.

Keywords

Plant root bacteria, Root exudates, Benzoxazinoids, Synthetic community, Metabolisation

54 # Introduction

55 Most multicellular organisms are closely associated with microbial communities, which
56 provide important functions to the host. Plant microbiomes function in promoting growth,
57 providing nutrients, protecting from disease but some microbiome members can also act as
58 pathogens (1–3). The microbial members including bacteria, fungi, protists and oomycetes co-
59 adapted with their host over long evolutionary time scales (4–7). Root exudates, which can
60 account for up to one-fifth of the plant's assimilated carbon (8) contain primary metabolites
61 including sugars, amino acids, organic acids and fatty acids, as well as secondary metabolites. The
62 latter, also called specialized metabolites, act in diverse ways to govern the interactions with the
63 plant's environment. Often these compounds have antimicrobial function, selecting adapted
64 microbes and thereby shaping the species-specific root microbiome (8–12). Examples include
65 glucosinolates, camalexins, triterpenes, and coumarins in *Arabidopsis thaliana* (9), the saponin
66 tomatine from tomato (13), and benzoxazinoids (14–18), diterpenoids (19), zealexins (20) and
67 flavonoids (21) in maize. While there is increasing knowledge how individual microbes react to
68 these compounds, it is largely unknown how they cope as communities with antimicrobial root
69 exudates.

70 Microbial community members not only co-evolved with their hosts but they also adapted
71 to interact efficiently with each other. On one hand they developed mechanisms to optimize their
72 fitness through competitive mechanisms such as the production of antimicrobial compounds
73 (22). On the other hand, some also adapted to profit from each other to efficiently use resources
74 and accomplish tasks which are not feasible as individuals (23, 24). For example, community
75 members might exchange metabolites to complement each other's biosynthetic pathways (25).
76 Such interactions cannot only improve community fitness but also alter final product distribution,
77 and give rise to new phenotypes without genetic modification (26). Microbes often cooperate to
78 degrade antimicrobials or pollutants (24, 27) or metabolize complex substrates (28). Examples
79 include the metabolization of the herbicide atrazine by an adapted four-strain consortium in
80 which one bacterium metabolized the herbicide to cyanuric acid, which then served as a carbon
81 source for the other community members (29). Or, another three-strain consortium converted
82 the herbicide linuron more efficiently in co-culture showing increased expression of the linuron
83 hydrolase (30). Also, the degradation of antibiotics by one community member affected the
84 community composition (31). While there are examples of how microbial communities cooperate
85 to degrade antimicrobial compounds and pollutants, little is known about how root microbiome
86 members interact to cope with antimicrobial plant metabolites.

87 Crops belonging to the family of sweet grasses (*Poaceae*) include maize, wheat and rye
88 produce benzoxazinoids as specialized metabolites (32, 33). These indole-derived alkaloids

89 mainly function in protecting the plant from insect pests and pathogens (32, 34, 35), providing
90 support in iron uptake (36) and structuring the root microbiomes by acting as selective
91 antimicrobials (11, 14–18). **Fig. S1** contains the full names and structures of all abbreviated
92 compounds mentioned in this study. DIMBOA-Glc is the main root-exuded benzoxazinoid of
93 maize (16), and its chemical fate in soil is well understood: Upon exudation, DIMBOA-Glc is
94 deglycosylated by microbe- and/or plant-derived enzymes (35) to form DIMBOA, which
95 spontaneously converts to more stable MBOA (37). In soil, MBOA has a half-life of a few days and,
96 when further metabolized by microbes to reactive aminophenols (35), MBOA can take three
97 different routes: route (I) is favoured under aerobic conditions forming aminophenoxazinones
98 such as AMPO through oxidation (38); route (II) results in acetamides such as HMPAA through
99 acetylation (39), or alternatively, route (III) yields malonic acids such as HMPMA through
100 acylation (39). Route I is probably most relevant for the rhizosphere, and the resulting AMPO
101 remains detectable in the soil of maize fields for up to a few months (37). Several bacterial isolates
102 were shown to metabolize MBOA to AMPO, which is mediated by the lactonase BxdA (40). Route
103 II was demonstrated for the soil fungus *Fusarium sambucus*, which metabolizes BOA to the
104 acetamide HMPAA (39). Following Route III, the maize seed endophytic fungus *Fusarium*
105 *verticillioides* converts BOA to the malonamic acid HPMA catalysed by a metallo-β-lactamase (41).
106 There is first evidence that benzoxazinoid metabolization routes vary when different microbes
107 interact. The fungus *Fusarium verticillioides* was co-cultured with the bacterium *Bacillus*
108 *mojavensis* in presence of BOA and metabolization was redirected from HMPAA to the
109 aminophenoxazinone APO (42). Hence benzoxazinoid metabolization in complex microbial
110 communities warrants further research, for instance to test if microbes metabolically redirect
111 benzoxazinoid degradation.

112 To study the mechanisms governing composition and functions of microbial communities
113 and their interactions with the host or the environment, synthetic communities (SynComs) are a
114 useful tool (43). A SynCom is a microbial community created by rationally mixing strains from a
115 collection from a specific environment. Strains can be added, eliminated, substituted or individual
116 strain functions manipulated, thereby allowing the detailed study of SynCom members, their
117 functions and the resulting community performance (45). Although, these reduced systems do
118 not accurately represent nature, they allow the replication of phenotypes mediated by the
119 microbiome.

120 Here we aimed to test if maize root bacteria interact to tolerate and metabolize the
121 benzoxazinoid MBOA in small SynComs. We investigated I) the type of degradation metabolites
122 produced by SynComs and which SynCom members are responsible for metabolization, II) how
123 the ability to metabolize benzoxazinoids affects community growth and tolerance, and III) if

124 MBOA shapes the composition of the two SynComs differently depending on their ability to
125 metabolize MBOA. To address these questions, we designed two SynComs consisting of six
126 common core strains and one variable *Microbacterium* strain that differed in the ability to
127 metabolize MBOA. We exposed the SynComs to MBOA and measured community growth,
128 community tolerance, community composition and benzoxazinoid metabolite profiles. We found
129 the SynCom containing the benzoxazinoid metabolizing *Microbacterium* to convert MBOA to
130 HMPAA, to grow on MBOA as a sole carbon source and to be more tolerant to MBOA. Interestingly,
131 the benzoxazinoid metabolite HMPAA was not formed by single strains but only in the SynCom in
132 combination of *Microbacterium* LMB2 with another strain. Our results revealed that maize root
133 bacteria interact to metabolize and tolerate benzoxazinoids, which is beneficial for microbial
134 growth.

135

136 Results

137 In community, the bacteria metabolize MBOA to HMPAA instead of AMPO

138 In previous work, we characterized individual maize root bacteria for their abilities to
139 tolerate (11) and metabolize benzoxazinoids (40). In this study, we investigated how these traits
140 function in a community context. To this end we examined growth and composition of a synthetic
141 community (SynCom) of maize root bacteria and the metabolites they produce after exposure to
142 MBOA. We constructed two 7-member SynComs consisting of taxonomically distinct bacteria
143 (distinguishable by 16S rRNA gene amplicon sequencing) that differed in their tolerance to MBOA
144 (**Fig. 1A, Fig. S2**). Both SynComs shared a common core of six bacteria that do not degrade MBOA
145 in liquid culture (see notes on LMX9231 in **Supplementary Results**, **Fig. S3**). To complete the
146 communities, alternative *Microbacterium* strain, differing in their ability to metabolize MBOA,
147 were added to each. This resulted in a *non*-metabolizing SynCom (nonSC) containing
148 *Microbacterium* LMI1x which is unable to metabolize MBOA, and a MBOA-*metabolizing* SynCom
149 (metSC) containing the MBOA degrader *Microbacterium* LMB2 (**Fig. 1A**). Importantly,
150 monocultures of *Microbacterium* LMB2 produce primarily AMPO after exposure to MBOA (**Fig.
151 S3B**).

152 To test community effects, we cultured the nonSC and metabolizing metSC in 96-well
153 plates in complex medium supplemented with 500 µM MBOA. We performed metabolite analyses
154 to confirm their differential MBOA degradation and to determine the various metabolization
155 products at 68 h (**Fig. S1, see Materials and Methods**). We found that the nonSC did not degrade
156 MBOA as expected whereas the metSC degraded MBOA and formed HMPAA rather than AMPO
157 (**Fig. 1B**). Over the course of the experiment, the levels of MBOA continuously decreased, HMPAA

158 continuously increased and not much AMPO accumulated (Fig. S4A). In addition, we also detected
159 a metabolite feature with a mass corresponding to the intermediate AMP (acetylation of AMP
160 yields HMPAA; Fig. S1) that accumulated over time similar to HMPAA (Fig. S4B). In summary,
161 the two SynComs nonSC and metSC differ in their ability to metabolize MBOA. In contrast to pure
162 cultures of LMB2 that primarily produce AMPO (Fig. S3B), we measured predominantly the
163 MBOA metabolization product HMPAA in the metSC where LMB2 is present in combination with
164 other strains. This finding indicates that *Microbacterium* LMB2 interacts with at least one other
165 metSC strain, resulting in the formation of HMPAA.

166 Most strains can form HMPAA together with LMB2

167 To identify the strain(s) that are involved in HMPAA formation, we first tested reduced
168 metSC communities in which individual strains were dropped out. We incubated these 'dropout
169 SynComs' in complex medium supplemented with 500 µM MBOA for 68 h and performed
170 metabolite analyses to determine the various metabolization products (Fig. S1). First, the
171 dropout SynCom without *Microbacterium* LMB2 did not degrade MBOA (Fig. 2A), confirming the
172 key role of LMB2 in initiating the metabolization of MBOA. Second, HMPAA was formed in all
173 other dropout SynComs in which another strain was removed. While the dropout of *Enterobacter*
174 LMX9231 and *Stenotrophomonas* LST17 did not markedly alter the metabolizing capacity of the
175 metSC, considerable levels of MBOA were still detected in the dropout SynComs lacking any of the
176 other four strains. Overall, this indicated that not one single specific strain is required for
177 formation of HMPAA in the metSC.

178 For further identification of individual strains interacting with *Microbacterium* LMB2 to
179 form HMPAA, we tested each community member paired with LMB2 as in the assay above.
180 Consistent with previous work (33; Fig. S3B), pure cultures of *Microbacterium* LMB2 completely
181 degraded MBOA and formed primarily AMPO (Fig. 2B). In co-cultures with *Bacillus* LBA21,
182 *Streptomyces* LMG1 and *Chitinophaga* LMN1, AMPO remained the primary product measured. In
183 contrast, in co-cultures with *Pseudomonas* LMX9, *Enterobacter* LMX9231 and *Stenotrophomonas*
184 LST17 little or no AMPO was detected, similar to the full metSC. Importantly, with the exception
185 of the co-culture with *Bacillus* LBA21, most pairs formed HMPAA. The highest levels of HMPAA
186 were detected in co-cultures with *Pseudomonas* LMX9 and *Stenotrophomonas* LST17,
187 intermediate levels with *Enterobacter* LMX9231 and the full metSC and low levels with
188 *Streptomyces* LMG1 and *Chitinophaga* LMN1. Taken together, HMPAA can be formed with five out
189 of the six core members of the metSC in co-culture with *Microbacterium* LMB2. According to the
190 chemical model (Fig. S1), we hypothesize that *Microbacterium* LMB2 initiates the metabolization
191 of MBOA by opening its lactone ring by BxdA (40) and forming the intermediate AMP, which can

192 then be further acetylated to HMPAA by each of these five strains. In absence of these strains, the
193 intermediate AMP undergoes oxidative dimerization to AMPO.

194 The metabolizing SynCom exhibits growth in the presence of MBOA

195 Next, we tested whether the ability to metabolize MBOA enables the metSC to use MBOA
196 as a sole carbon source for bacterial growth. For this we grew the nonSC and metSC SynComs in
197 minimal media supplemented with 500 or 2'500 µM MBOA, glucose (Glc) or no additional carbon
198 source (DMSO), keeping the DMSO concentration between treatments constant. We quantified
199 community growth by monitoring optical density (OD_{600}) over time. While both SynComs
200 exhibited similar growth in the DMSO and glucose controls, the metSC grew significantly better
201 in MBOA than the nonSC, particularly at the high MBOA concentration (**Fig. 3**). Testing all strains
202 individually confirmed that *Microbacterium* LMB2 was the only strain capable of utilizing MBOA
203 as a sole carbon source (**Fig. S5**). This analysis suggested that the metabolizing SynCom metSC
204 benefitted from LMB2's capacity to use MBOA as a sole carbon source. Of note, this conclusion
205 comes with the caveat that the OD_{600} measurements do not discriminate between the growth of
206 LMB2 and the other community members (see below).

207 The capacity to metabolize MBOA affects community size and structure

208 To examine the effect of the MBOA metabolization trait on community size, we next
209 exposed both SynComs in complex medium to 500 or 2'500 µM of MBOA or a control treatment
210 (DMSO) for 68 h. For scale and sampling reasons we performed this experiment in Erlenmeyer
211 flasks and first confirmed that MBOA was degraded by the metSC but not by the nonSC in this
212 experimental setting and that HMPAA is also the dominant degradation product under these
213 conditions (**Fig. S6A&B**). We found that the total community size, as determined by colony-
214 forming units (CFU), decreased with increasing levels of MBOA but that the metSC showed a
215 larger community size than the nonSC in presence of MBOA (**Fig. 4A**). Complementary, we also
216 determined the OD_{600} of the cultures and found similar results (**Fig. S6C**), with both CFU- and OD-
217 based community quantifications correlating well (**Fig. S6D**). This revealed that the ability to
218 metabolize MBOA enabled the metSC community to reach a higher population size when faced
219 with the antimicrobial compound.

220 In the same experiment, we also determined community compositions of the two SynComs using
221 amplicon sequencing. While the presence of MBOA significantly affected community composition
222 (PERMANOVA, $R^2 = 0.26$, $P = 0.001$), no major effect was found for the two types of SynComs or
223 their interaction with MBOA (**Table S1**). Constrained ordination visualized this MBOA effect
224 along the first axis with SynCom compositions differing at the high MBOA concentration relative
225 to communities at 500 µM MBOA and the DMSO controls (**Fig. 4B**). The high MBOA treatment

226 (2'500 µM) had a stronger impact on the composition of the nonSC than on the metSC. In DMSO
227 and at 500 µM of MBOA, both SynComs were compositionally dominated by *Stenotrophomonas*
228 LST17, followed by lower levels of *Enterobacter* LMX9231 and *Chitinophaga* LMN1 while the
229 other strains were either only detected at very low levels or not any more (**Fig. 4C**, **Fig. S7A**).
230 Comparisons to the input samples collected at SynCom assembly, confirmed that all strains were
231 present in the initial SynComs (**Fig. S7B**). While the composition of the metSC was more similar
232 compared to the control and 500 µM MBOA treatments, several core strains of both SynComs
233 differed in their relative abundances at high MBOA levels: *Stenotrophomonas* LST17 (susceptible
234 to MBOA; tolerance from **Fig. 1A** and **S2**), which made up about 70% of the community in the
235 DMSO and MBOA 500 µM treatment, was strongly reduced to 22% and 47% in the nonSC and
236 metSC, respectively. In contrast, *Enterobacter* LMX9231 (intermediate tolerance) and
237 *Pseudomonas* LMX9 (tolerant), as well as *Chitinophaga* LMN1 (susceptible) increased in their
238 relative abundances at high MBOA concentration relative to the DMSO and 500 µM treatments. In
239 conclusion, MBOA reduces bacterial community size (**Fig. 4A**), and influences community
240 composition more strongly if a SynCom is unable to metabolize the compound (**Fig. 4B&C**).

241

242 Discussion

243 Root-derived plant specialized metabolites structure microbiomes (9) and select root-
244 associated bacteria that can both tolerate (11) and/or metabolize (40) these compounds. In this
245 study we found that maize root bacteria, assembled as a synthetic community, interacted to
246 metabolize benzoxazinoids *in vitro,* leading to the accumulation of the alternative MBOA-
247 metabolization product HMPAA. The capacity to metabolize benzoxazinoids appeared to be
248 beneficial to the metSC SynCom, enhancing the tolerance to MBOA and enabling the community
249 to reach higher population densities than the nonSC SynCom at high MBOA concentrations.
250 Furthermore, the effect of MBOA on community composition was dependent on the
251 metabolization phenotype. Below we discuss the underlying mechanisms and benefits for
252 microbial communities.

253 Interacting bacteria redirect BX metabolism

254 Members of microbial communities often interact to degrade complex chemicals such as
255 antimicrobial compounds, pollutants, and complex substrates but also cooperate for substrate
256 utilization (24). Here, we found that SynComs of maize root bacteria interacted in the
257 metabolization of MBOA. Against the expectation from our previous study, where we reported
258 that single-strain cultures of *Microbacterium* LMB2 metabolized MBOA to AMPO (40), we found
259 that the MBOA metabolizing metSC SynCom formed HMPAA as a dominant metabolite. Since none

260 of the metSC strains formed HMPAA in single-strain culture, we concluded that HMPAA formation
261 required the sole MBOA-degrading bacterium *Microbacterium* LMB2 in combination with at least
262 one other strain. In paired cultures *Pseudomonas* LMX9 had the strongest effect of MBOA
263 degradation and lead to complete AMPO absence, thus this strain appears to be the strongest
264 contributor among the SynCom strains. Similar alternative product formation during
265 benzoxazinoid degradation has previously been reported for a co-culture of the fungus *Fusarium*
266 *verticillioides* with the bacterium *Bacillus mojavensis* (42). The *Fusarium* alone metabolized BOA
267 to HMPA, but in co-culture with *Bacillus*, the intermediate AP was oxidized to the APO. Since the
268 *Fusarium* is susceptible to APO while the *Bacillus* is not, this metabolic interaction resulted in
269 inhibition of the pathogenic fungus without negatively affecting the bacterium. Here, we found
270 that interacting bacteria redirected benzoxazinoid metabolization to an alternative compound.

271 ## Mechanism of alternative MBOA metabolization

272 The formation of the alternative MBOA metabolization product HMPAA by the metSC
273 SynCom required at least two strains and was only observed when *Microbacterium* LMB2 was
274 present. Therefore, it is likely that LMB2 degraded MBOA by the previously identified lactonase
275 BxdA (40) to the intermediate AMP, which is then acetylated by a second strain to HMPAA. There
276 is evidence pointing towards such an acetylation as second step: *Pseudomonas chlororaphis* for
277 example possesses an arylamine N-acetyltransferase (NAT1) that acetylates AP to AAP (47). It is
278 possible that some SynCom strains possess homologues of NAT1 which analogously could act on
279 AMP, a methoxylated AP, resulting in HMPAA formation. Further genomic and functional work
280 with knockouts and transcriptomics is required to confirm the role of NAT1 homologs in HMPAA
281 formation. Alternatively, a second pathway was proposed for the production of the acetamide
282 AAP: acylation of AP to the malonylated form HMPA followed by deacetylation to AAP (48).
283 Detoxification of benzoxazinoids via ring-opening and malonylation is well-known for fungal
284 pathogens such as *Fusarium* species (41, 49). Throughout our analyses, we did not detect the
285 malonylated intermediate HMPMA. However, as HPMA can be degraded by microorganisms such
286 as Bacilli with and without the accumulation of AAP (48), the absence of HMPMA might also be
287 explained by further degradation of such a product. Future work will focus on the identification
288 and characterization of homologs of arylamine N-acyltransferases in the tested SynCom strains.
289 *Pseudomonas* LMX9 will be especially interesting in this regard as it is the only strain that led to
290 complete absence of AMPO in paired culture with *Microbacterium* LMB2 and also seemed to have
291 the strongest effect on MBOA degradation in single dropouts of the metSC (**Fig. 2**). Our
292 benzoxazinoid metabolizing SynCom thus offers a great tool to disentangle the biochemistry of
293 bacterial interaction for metabolization of plant specialized metabolites.

294 ## Interaction in benzoxazinoid metabolization is beneficial to community fitness

295 Benzoxazinoids were shown to selectively inhibit bacterial growth (11, 50), are
296 metabolized by individual bacterial members of the maize root microbiome (40–42) and alter the
297 composition of root microbial communities (14–16). Here we found that the metSC SynCom was
298 more tolerant to MBOA than the nonSC SynCom (**Fig. 4A**). MBOA not only altered the size but also
299 the composition of both SynComs implying that certain strains were more affected by the
300 presence of MBOA than others (**Fig. 4C**). Specifically, high MBOA concentrations strongly reduced
301 *Stenotrophomonas* LST17, which dominated the SynComs containing no or low amounts of MBOA,
302 whereas *Pseudomonas* LMX9 and *Chitinophaga* LMN1 increased in relative abundance at the high
303 MBOA concentrations. It is currently unclear, whether this increase in LMX9 and LMN1 was due
304 to an increase in absolute abundance or whether the abundance of the strains remained stable
305 and relative abundance solely increased due to the reduction of *Stenotrophomonas* LST17. For
306 LST17, the inhibition was linked to its low tolerance to high concentrations of MBOA (**Fig. S2**). In
307 the metSC SynCom, the *Stenotrophomonas* remained the most abundant strain, which could be
308 explained by MBOA degradation and implies that this strain was also tolerant to the produced
309 HMPAA.

310 It is currently unclear how the population dynamics developed over the course of the
311 experiment. Even though *Microbacterium* LMB2 is required for MBOA metabolization in the
312 metSC, it was only detected at low concentrations at the end of the experiment. One possible
313 explanation is that LMB2 was present at higher concentrations at the beginning of the
314 experiment, but then after initiating the MBOA metabolization, it was overgrown by fast-growing
315 and less MBOA tolerant strains. In line with this, *Stenotrophomonas* LST17 would have been first
316 present at low abundance and then started growing once MBOA concentrations fell below
317 inhibitory concentrations. Interestingly, *Chitinophaga* LMN1 that also showed hardly any growth
318 at 2'500 µM MBOA *in vitro* increased stronger in relative abundance in the nonSC than in the
319 metSC at high MBOA. This suggested that other factors than MBOA tolerance contributed to the
320 final SynCom composition such as microbe-microbe interactions based on metabolic exchanges
321 between SynCom strains or modulation of direct competitive interactions (51, 52). Cross-feeding
322 was for example previously identified in a 7-member community of maize root bacteria (53). An
323 *Enterobacter* had previously been identified as keystone species in this SynCom (54). The
324 keystone *Enterobacter* had the broadest substrate utilization of maize root extracts and its
325 dropout decreased carbohydrate utilization of the SynCom (53). Our SynCom also contained an
326 *Enterobacter* showing high abundance and substrate use may further explain community
327 structure independent of tolerance to benzoxazinoids. Nevertheless, our observation that
328 benzoxazinoids structured SynComs also *in vitro*, underlines the importance of benzoxazinoids

329 in shaping root-associated microbial communities on benzoxazinoid producing maize roots (14–
330 17).

331 Effect of benzoxazinoid metabolization for bacterial growth and potential effects on host
332 health

333 It remains an open question why microbes metabolize benzoxazinoids. Whether it is to
334 detoxify them, to profit from a carbon source, to use degradation products as defence against
335 other microbiota members or whether degradation is beneficial for the host. We found that a
336 benzoxazinoid metabolizing SynCom was more tolerant to MBOA at high MBOA concentrations,
337 which suggests specific adaption of host microbiomes to tolerate and metabolize host specialized
338 metabolites and potentially presents a strategy for rhizosphere bacteria to access an extra carbon
339 source to thrive in the rhizosphere (53, 55). Indeed, MBOA can be used as a sole carbon source by
340 the degrading *Microbacterium* LMB2 (40). However, our SynCom experiments in complex
341 medium suggest that under the tested conditions MBOA metabolization served mainly for
342 detoxification for some microbiome members rather than strongly contributing to overall
343 population size as a separate carbon source. As degradation of specialized metabolites can be
344 highly context and environment dependent, the SynCom work could be next transferred to a
345 gnotobiotic plant system as tested by Niu et al. (54). Members of the genus *Stenotrophomonas*
346 show beneficial effects for plant growth and health (56). In a first step one could therefore focus
347 on whether presence of MBOA metabolization increases local *Stenotrophomonas* abundance also
348 *in planta* and potentially affects SynCom functions supplied to the host such as protection against
349 plant pathogens. Alternatively, benzoxazinoid degradation and degradation products could
350 additionally influence community function as regulators (57). Given the widespread nature of
351 microbial interactions and the diversity of plant specialized metabolites, we propose that
352 microbial interactions affect how microbial communities cope with plant specialized metabolites
353 across the plant kingdom and thereby also potentially influence plant fitness.

354 Conclusion

355 Natural microbial communities are diverse and single members interact to fulfil a
356 complex task or to use resources efficiently (24). Here we report that maize root bacteria interact
357 to tolerate and metabolize benzoxazinoids. Especially at high benzoxazinoid concentrations, the
358 interaction of maize root bacteria positively affected the performance as a community. Our
359 findings highlight the importance of studying plant specialized metabolites mediating chemical
360 communication in plant-microbiome interactions in more complex synthetic or natural microbial
361 communities.

362

363 # Materials and Methods

364 ## Bacteria, SynCom assembly and experimental setup

365 Maize root bacteria (i.e., MRB collection) (11) were routinely grown on solid 100% TSA
366 plates (30 g/L tryptic soy broth and 15 g/L of agar, both Sigma-Aldrich) or in liquid 50% TSB
367 medium (15 g/L tryptic soy broth) with 180 rpm shaking at 25 – 28 °C. For cryo stocks, bacteria
368 were grown for 48 h in liquid 100% TSB (30 g/L tryptic soy broth) and mixed with sterile-filtered
369 glycerol (Sigma-Aldrich) at a final concentration of 20%.

370 The SynComs were assembled from taxonomically different MRB strains (11) that are
371 distinguishable by 16S rRNA gene amplicon sequencing and differ in their ability to metabolize
372 MBOA on their own (40). The SynComs were composed of the following six core strains, which
373 do not metabolize MBOA: *Stenotrophomonas* LST17, *Pseudomonas* LMX9, *Enterobacter* LMX9231,
374 *Chitinophaga* LMN1, *Bacillus* LBA21, *Streptomyces* LMG1. With the seventh strain, the SynComs
375 differed in their ability to metabolize MBOA: *Microbacterium* LMI1x is unable to metabolize MBOA
376 and was selected for the *non*-metabolizing SynCom (nonSC). *Microbacterium* LMB2 metabolizes
377 MBOA on its own to AMPO and was part of the MBOA-*metabolizing* SynCom (metSC).

378 The individual strains were pre-grown in liquid cultures for the different experiments.
379 For experiments depicted in Figs 1-3, pre-cultures were inoculated from single colonies and
380 grown in 1 mL of liquid 50% TSB in 2 mL 96-well deep-well plates (Semadeni, Ostermundigen,
381 Switzerland). Pre-culture plates were covered with a Breathe-Easy membrane (Diversified
382 Biotech, Dedham, USA) and grown until stationary phase for 4 days at 28°C and 180 rpm.

383 For preparation of SynComs or strain mixes, cultures of individual strains were adjusted
384 to OD_{600} = 0.6 and the required strains mixed at equal ratios. Main cultures were inoculated by
385 adding 4 µL of the adjusted mixes/single strains into 96-well microtiter plates (Corning, Corning,
386 USA) containing 200 µL of fresh liquid media including the compounds at the concentrations to
387 be tested. The chemical treatments were prepared at the desired concentrations by mixing their
388 stock solutions into the liquid growth media. The stock solution for MBOA (Sigma-Aldrich) was
389 prepared in the solvent DMSO (Sigma-Aldrich) at 606 mM (100 mg/mL). MBOA was added to the
390 medium at final concentrations of 0, 500 or 2'500 µM and the DMSO concentration was kept
391 constant in all treatments including the controls.

392 We mainly utilized our previously described 96-well liquid culture based growth system
393 (11). In brief, bacterial growth was monitored in 96-well plates in a high-throughput manner
394 using a stacker (BioStack 4, Agilent Technologies, Santa Clara, USA), which was connected to a
395 plate reader (Synergy H1, Agilent Technologies, Santa Clara, USA). This system shakes the
396 cultures for 2 min (approx. every 80 minutes) before recording the OD_{600} readings in the plate

397 reader. In each plate, wells with growth medium were included as no bacteria controls (NBC) and
398 in each run one plate containing only media was included to monitor potential contaminations.
399 For assessing community structure, precultures and SynComs were grown in Erlenmeyer flasks
400 instead of 96-well plates and growth was assessed by OD_{600} measurements using a
401 biophotometer (Eppendorf, Hamburg, Germany) and by dilution series plating and colony-
402 forming units determination.

403 For details on the different experiments performed see **Supplementary Methods**.

404 **Data analysis:** We used the R version 4.0 (R core Team, 2016) for all statistical analysis and
405 visualization of the data. We first inspected the bacterial growth data for normality using Shapiro-
406 Wilk tests. Differences between the two SynComs (nonSC vs. metSC) and treatments were
407 assessed using pairwise t-tests and reported for the different treatments in the graphs. P-values
408 were adjusted for multiple hypothesis testing using the Bonferroni method within R. We used the
409 following packages for data analysis and visualizations: Tidyverse (58), Broom (59), DECIPHER
410 (60), DESeq2 (61), emmeans (62), ggthemes (63), pheatmap (64), multcomp (65), phyloseq (66),
411 phytools (67), vegan (68) in combination with custom functions. All source data and R code used
412 for statistical analysis and graphing are available from https://github.com/PMI-
413 Basel/Thoenen_et_al_SynCom.

414 Metabolite analysis from bacterial cultures

415 Samples for metabolite analyses were processed and measured as described previously
416 (40). Briefly, metabolites in bacterial cultures were fixed in 70% MeOH + 0.1% FA. Replicates of
417 the same sample group were pooled and diluted followed by filtration and centrifugation to
418 remove bacterial debris. Benzoxazinoids and their degradation products were profiled using an
419 Acquity I-Class UHPLC system (Waters, Milford, USA) coupled to a Xevo G2-XS QTOF mass
420 spectrometer (Waters, Milford, USA) equipped with a LockSpray dual electrospray ion source
421 (Waters, Milford, USA). Different benzoxazinoid standard compounds were run together with the
422 samples at varying concentrations and used for quantification and identification. Here in this
423 work, we only report MBOA, AMPO and HMPAA. For details see Supplementary Methods. All
424 source data and R code used for graphing are available from https://github.com/PMI-
425 Basel/Thoenen_et_al_SynCom.

426 Community analysis

427 DNA was extracted from 1 mL of SynCom samples (Experiment 4) using the NucleoSpin
428 Soil kit (Macherey-Nagel, Düren, Germany) following the manufacturer's instructions (see also
429 **Supplementary Methods**). The 16S rRNA gene was amplified in a two-step PCR, with custom
430 barcodes for sample identification added in the second PCR. The detailed method for PCR

amplification and their primers, product purification and pooling is described in the **Supplementary Methods**. The pooled library was sequenced on a MiSeq instrument (Illumina Inc., San Diego, USA) with a v2 nano flow cell and the 2x250 bp pair-end sequencing protocol at the Next Generation Sequencing Platform (https://www.ngs.unibe.ch, University of Bern, Switzerland). The raw sequencing data was deposited at the European Nucleotide Archive (http://www.ebi.ac.uk/ena) under project number PRJEB86484.

The raw sequencing data were processed in R using the DADA2 pipeline version 1.20 (69). For details see **Supplementary Methods.** The 16S rRNA gene sequences of the SynCom members were mapped to the amplicon sequences using usearch (70) with an identity of 0.97. The counts of the mapped ASVs were normalized by rarefaction using phyloseq (66) and the abundances of the strains were further adjusted based on their estimated copy numbers of the 16S rRNA genes (**Dataset S1**). Compositional differences between the SynComs and by the treatments were assessed using Permutational Analysis of Variance (PERMANOVA, 99'999 permutations; model: ~ SynCom * Treatment) on Bray Curtis distances using the R package vegan (68). The effects on community composition using the same model were visualized with a Canonical Analysis of Principal Coordinates (CAP) using the R package phyloseq (66). All source data and code used for statistical analysis and graphing are available from https://github.com/PMI-Basel/Thoenen_et_al_SynCom.

Data availability

All source data is made publicly available. The sequencing data is available from the European Nucleotide Archive as Bioproject PRJEB86484. We provide all data on bacterial growth and metabolite data together with their analysis code on GitHub (https://github.com/PMI-Basel/Thoenen_et_al_SynCom).

Code availability

All code used for statistical analysis and graphing is available from GitHub (https://github.com/PMI-Basel/Thoenen_et_al_SynCom).

Acknowledgments

We thank Corinne Suter for support with culturing bacteria and plating assays and Mirco Hecht for supporting metabolomic analysis. Further, we thank Dr. Thomas Roder for the support with the open genome browser, Dr. Pamela Nicholson from the Next Generation Sequencing Platform in Bern for technical support with sequencing. This work was mainly supported by the Interfaculty Research Collaboration "One Health" of the University of Bern. It has also received support by grants of the European Research Council (No. 949595 to C.R.) and the Swiss National Science Foundation (No. 189071 to C.R.). Finally, the work was supported by the State Secretariat for Education, Research and Innovation SERI-funded ERC Consolidator Grant "mifeePs" (No. M822.00079 to K.S.).

470 ## References

471 1. Bulgarelli D, Schlaeppi K, Spaepen S, van Themaat EVL, Schulze-Lefert P. 2013. Structure
472 and functions of the bacterial microbiota of plants. Annual Review of Plant Biology
473 64:807–838.

474 2. Mendes R, Garbeva P, Raaijmakers JM. 2013. The rhizosphere microbiome: significance of
475 plant beneficial, plant pathogenic, and human pathogenic microorganisms. Fems
476 Microbiology Reviews 37:634–663.

477 3. Trivedi P, Leach JE, Tringe SG, Sa T, Sa T, Singh BK. 2020. Plant–microbiome interactions:
478 from community assembly to plant health. Nature Reviews Microbiology 18:607–621.

479 4. Baumann P. 2005. BIOLOGY OF BACTERIOCYTE-ASSOCIATED ENDOSYMBIONTS OF
480 PLANT SAP-SUCKING INSECTS. Annual Review of Microbiology 59:155–189.

481 5. Ley RE, Hamady M, Lozupone CA, Turnbaugh PJ, Ramey RR, Bircher JS, Schlegel ML, Tucker
482 TA, Schrenzel MD, Knight R, Gordon JI. 2008. Evolution of mammals and their gut
483 microbes. Science 320:1647–1651.

484 6. Sprent JI. 2007. 60Ma of legume nodulation. What's new? What's changing? Journal of
485 Experimental Botany 59:1081–1084.

486 7. Escudero-Martinez C, Bulgarelli D. 2019. Tracing the evolutionary routes of plant–
487 microbiota interactions. Current Opinion in Microbiology 49:34–40.

488 8. Sasse J, Martinoia E, Northen TR. 2018. Feed Your Friends: Do Plant Exudates Shape the
489 Root Microbiome? Trends in Plant Science 23:25–41.

490 9. Jacoby RP, Koprivova A, Kopriva S. 2020. Pinpointing secondary metabolites that shape the
491 composition and function of the plant microbiome. Journal of Experimental Botany 72:57–
492 69.

493 10. Lareen A, Burton F, Schäfer P. 2016. Plant root-microbe communication in shaping root
494 microbiomes. Plant Molecular Biology 90:575–587.

495 11. Thoenen L, Giroud C, Kreuzer M, Waelchli J, Gfeller V, Deslandes-Hérold G, Mateo P, Robert
496 CAM, Ahrens CH, Rubio-Somoza I, Bruggmann R, Erb M, Schlaeppi K. 2023. Bacterial
497 tolerance to host-exuded specialized metabolites structures the maize root microbiome.
498 Proc Natl Acad Sci USA 120:e2310134120.

499 12. Stringlis IA, Yu K, Feussner K, de Jonge R, van Bentum S, Van Verk MC, Berendsen RL,
500 Bakker PAHM, Feussner I, Pieterse CMJ. 2018. MYB72-dependent coumarin exudation
501 shapes root microbiome assembly to promote plant health. Proceedings of the National
502 Academy of Sciences of the United States of America 115:5213–5222.

503 13. Nakayasu M, Ohno K, Takamatsu K, Yuichi Aoki, Aoki Y, Yamazaki S, Takase H, Shoji T,
504 Yazaki K, Sugiyama A. 2021. Tomato roots secrete tomatine to modulate the bacterial
505 assemblage of the rhizosphere. Plant Physiology 186:270–284.

506 14. Cadot S, Guan H, Bigalke M, Walser J-C, Jander G, Erb M, van der Heijden MGA, Schlaeppi K.
507 2021. Specific and conserved patterns of microbiota-structuring by maize benzoxazinoids
508 in the field. Microbiome 9:103–103.

509 15. Cotton TEA, Pétriacq P, Cameron DD, Meselmani MA, Schwarzenbacher RE, Rolfe SA, Ton J.
510 2019. Metabolic regulation of the maize rhizobiome by benzoxazinoids. The ISME Journal
511 13:1647–1658.

512 16. Hu L, Robert CAM, Cadot S, Zhang X, Ye M, Li B, Daniele Manzo, Manzo D, Chervet N,
513 Steinger T, Thomas Steinger, van der Heijden MGA, Schlaeppi K, Erb M. 2018. Root exudate
514 metabolites drive plant-soil feedbacks on growth and defense by shaping the rhizosphere
515 microbiota. Nature Communications 9:2738–2738.

516 17. Kudjordjie EN, Sapkota R, Steffensen SK, Fomsgaard IS, Nicolaisen M. 2019. Maize
517 synthesized benzoxazinoids affect the host associated microbiome. Microbiome 7:59–59.

518 18. Schütz V, Frindte K, Cui J, Zhang P, Hacquard S, Schulze-Lefert P, Knief C, Schulz M,
519 Dörmann P. 2021. Differential Impact of Plant Secondary Metabolites on the Soil
520 Microbiota. Frontiers in Microbiology 12:666010.

521 19. Murphy KM, Edwards J, Louie KB, Bowen BP, Sundaresan V, Northen TR, Zerbe P. 2021.
522 Bioactive diterpenoids impact the composition of the root-associated microbiome in maize
523 (Zea mays). Scientific Reports 11:333.

524 20. Ding Y, Weckwerth PR, Poretsky E, Murphy KM, Sims J, Saldivar E, Christensen SA, Char SN,
525 Yang B, Tong A dao, Shen Z, Kremling KA, Buckler ES, Kono TJY, Nelson DR, Bohlmann J,
526 Bakker MG, Bakker MG, Bakker MG, Vaughan MM, Khalil AS, Betsiashvili M, Dressano K,
527 Köllner TG, Briggs SP, Zerbe P, Schmelz EA, Huffaker A. 2020. Genetic elucidation of
528 interconnected antibiotic pathways mediating maize innate immunity. Nature plants
529 6:1375–1388.

530 21. Yu P, He X, Baer M, Beirinckx S, Tian T, Moya YAT, Zhang X, Deichmann M, Frey FP, Bresgen
531 V, Li C, Razavi BS, Schaaf G, von Wirén N, Su Z, Bucher M, Tsuda K, Goormachtig S, Chen X,
532 Chen X, Chen X, Hochholdinger F. 2021. Plant flavones enrich rhizosphere
533 Oxalobacteraceae to improve maize performance under nitrogen deprivation. Nature
534 plants 7:481–499.

535 22. García-Bayona L, Comstock LE. 2018. Bacterial antagonism in host-associated microbial
536 communities. Science 361:eaat2456.

537 23. Bardone E, Marzocchella A, Bravi M, Gómez-Camacho CE, Ruggeri B. 2020. Microbial
538 Engineering Community (MCE): Selecting Key Players in Microbiomes.

539 24. Rafieenia R, Atkinson E, Ledesma-Amaro R. 2022. Division of labor for substrate utilization
540 in natural and synthetic microbial communities. Current Opinion in Biotechnology
541 75:102706–102706.

542 25. Ponomarova O, Patil KR. 2015. Metabolic interactions in microbial communities:
543 untangling the Gordian knot. Current Opinion in Microbiology 27:37–44.

544 26. Diender M, Olm IP, Sousa DZ. 2021. Synthetic co-cultures: novel avenues for bio-based
545 processes. Current Opinion in Biotechnology 67:72–79.

546 27. Qi M, Liang B, Liang B, Long Zhang, Zhang L, Ma X, Yan L, Dong W, Dong W, Kong D, Zhang
547 L, Zhu H, Gao S-H, Jiang J-D, Jiang J, Liu S-J, Corvini PF-X, Wang A. 2021. Microbial
548 Interactions Drive the Complete Catabolism of the Antibiotic Sulfamethoxazole in
549 Activated Sludge Microbiomes. Environmental Science & Technology 55:3270–3282.

550 28. McCarty NS, Ledesma-Amaro R. 2019. Synthetic Biology Tools to Engineer Microbial
551 Communities for Biotechnology. Trends in Biotechnology 37:181–197.

552 29. Billet L, Marion Devers, Devers M, Rouard N, Martin-Laurent F, Spor A. 2019. Labour
553 sharing promotes coexistence in atrazine degrading bacterial communities. Scientific
554 Reports 9:18363.

555 30. Albers P, Weytjens B, De Mot R, Marchal K, Kathleen Marchal, Springael D. 2018. Molecular
556 processes underlying synergistic linuron mineralization in a triple-species bacterial
557 consortium biofilm revealed by differential transcriptomics. MicrobiologyOpen 7.

558 31. Pathak A, Angst DC, León-Sampedro R, Hall AR. 2023. Antibiotic-degrading resistance
559 changes bacterial community structure via species-specific responses. The ISME Journal
560 17:1495–1503.

561 32. Niemeyer HM. 2009. Hydroxamic acids derived from 2-hydroxy-2H-1,4-benzoxazin-3(4H)-
562 one: key defense chemicals of cereals. Journal of Agricultural and Food Chemistry
563 57:1677–1696.

564 33. Wouters FC, Blanchette B, Gershenzon J, Vassão DG. 2016. Plant defense and herbivore
565 counter-defense: benzoxazinoids and insect herbivores. Phytochemistry Reviews
566 15:1127–1151.

567 34. Robert CAM, Veyrat N, Glauser G, Marti G, Doyen GR, Villard N, Gaillard MDP, Köllner TG,
568 Giron D, Body MJA, Babst BA, Ferrieri RA, Turlings TCJ, Erb M. 2012. A specialist root
569 herbivore exploits defensive metabolites to locate nutritious tissues. Ecology Letters
570 15:55–64.

571 35. Robert CAM, Mateo P. 2022. The Chemical Ecology of Benzoxazinoids. Chimia 76:928.

572 36. Hu L, Mateo P, Ye M, Zhang X, Berset JD, Berset JD, Handrick V, Radisch D, Grabe V, Köllner
573 TG, Gershenzon J, Robert CAM, Erb M. 2018. Plant iron acquisition strategy exploited by an
574 insect herbivore. Science 361:694–697.

575 37. Macías FA, Oliveros-Bastidas A, Marín D, Castellano D, Simonet and AM, Molinillo JMG.
576 2004. Degradation Studies on Benzoxazinoids. Soil Degradation Dynamics of 2,4-
577 Dihydroxy-7-methoxy-(2H)-1,4-benzoxazin-3(4H)-one (DIMBOA) and Its Degradation
578 Products, Phytotoxic Allelochemicals from Gramineae. Journal of Agricultural and Food
579 Chemistry 52:6402–6413.

580 38. Guo S, Hu H, Wang W, Bilal M, Zhang X. 2022. Production of Antibacterial Questiomycin A
581 in Metabolically Engineered Pseudomonas chlororaphis HT66. Journal of Agricultural and
582 Food Chemistry https://doi.org/10.1021/acs.jafc.2c03216.

583 39. Zikmundová M, Drandarov K, Bigler L, Hesse M, Werner C. 2002. Biotransformation of 2-
584 benzoxazolinone and 2-hydroxy-1,4-benzoxazin-3-one by endophytic fungi isolated from
585 Aphelandra tetragona. Applied and Environmental Microbiology 68:4863–4870.

586 40. Thoenen L, Kreuzer M, Pestalozzi C, Florean M, Mateo P, Züst T, Wei A, Giroud C, Rouyer L,
587 Gfeller V, Notter MD, Knoch E, Hapfelmeier S, Becker C, Schandry N, Robert CAM, Köllner
588 TG, Bruggmann R, Erb M, Schlaeppi K. 2024. The lactonase BxdA mediates metabolic
589 specialisation of maize root bacteria to benzoxazinoids. Nature Communications 15:6535.

590 41. Glenn AE, Davis CB, Gao M, Scott E. Gold, Scott E. Gold, Scott E. Gold, Gold SE, Mitchell TR,
591 Proctor RH, Stewart J, Stewart JE, Jane E. Stewart, Snook ME. 2016. Two Horizontally
592 Transferred Xenobiotic Resistance Gene Clusters Associated with Detoxification of
593 Benzoxazolinones by Fusarium Species. PLOS ONE 11.

594 42. Bacon CW, Hinton DM, Glenn AE, Macías FA, Marín D. 2007. Interactions of Bacillus
595 mojavensis and Fusarium verticillioides with a benzoxazolinone (BOA) and its
596 transformation product, APO. Journal of Chemical Ecology 33:1885–1897.

597 43. Vorholt JA, Vogel C, Carlström CI, Müller DB. 2017. Establishing Causality: Opportunities of
598 Synthetic Communities for Plant Microbiome Research. Cell Host & Microbe 22:142–155.

599 44. Bai Y, Müller DB, Srinivas G, Garrido-Oter R, Potthoff E, Rott M, Dombrowski N, Münch PC,
600 Spaepen S, Remus-Emsermann MNP, Hüttel B, McHardy AC, Vorholt JA, Schulze-Lefert P.
601 2015. Functional overlap of the Arabidopsis leaf and root microbiota. Nature 528:364–
602 369.

603 45. O'Banion B, O'Neal L, Alexandre G, Lebeis SL. 2020. Bridging the Gap Between Single-Strain
604 and Community-Level Plant-Microbe Chemical Interactions. Molecular Plant-microbe
605 Interactions 33:124–134.

606 47. Guo S, Wang Y, Wei Wang, Wang W, Wei Wang, Wang W, Hu H, Zhang X. 2020.
607 Identification of new arylamine N-acetyltransferases and enhancing 2-acetamidophenol
608 production in Pseudomonas chlororaphis HT66. Microbial Cell Factories 19:1–10.

609 48. Schütz V, Bigler L, Girel S, Laschke L, Sicker D, Schulz M. 2019. Conversions of
610 Benzoxazinoids and Downstream Metabolites by Soil Microorganisms. Frontiers in
611 Ecology and Evolution 7.

612 49. de Lima DP, dos Santos E dos A, Marques MR, Giannesi GC, Beatriz A, Yonekawa MKA,
613 Montanholi A dos S. 2018. Fungal bioremediation of pollutant aromatic amines. Current
614 Opinion in Green and Sustainable Chemistry 11:34–44.

615 50. Machado RAR, Thönen L, Arce CCM, Theepan V, Prada F, Prada F, Prada F, Wüthrich D,
616 Robert CAM, Vogiatzaki E, Shi Y-M, Schaeren OP, Notter MD, Bruggmann R, Hapfelmeier S,
617 Bode HB, Erb M. 2020. Engineering bacterial symbionts of nematodes improves their
618 biocontrol potential to counter the western corn rootworm. Nature Biotechnology 38:600–
619 608.

620 51. Pacheco AR, Vorholt JA. 2023. Resolving metabolic interaction mechanisms in plant
621 microbiomes. Current Opinion in Microbiology 74:102317.

622 52. Chepsergon J, Moleleki LN. 2023. Rhizosphere bacterial interactions and impact on plant
623 health. Current Opinion in Microbiology 73:102297.

624 53. Krumbach J, Patrizia Kroll, Wewer V, Metzger S, Till Ischebeck, Jacoby RP. 2021. Metabolic
625 analysis of a bacterial synthetic community from maize roots provides new mechanistic
626 insights into microbiome stability. bioRxiv https://doi.org/10.1101/2021.11.28.470254.

627 54. Niu B, Paulson JN, Zheng X, Kolter R. 2017. Simplified and representative bacterial
628 community of maize roots. Proceedings of the National Academy of Sciences of the United
629 States of America 114:201616148.

630 55. Huang AC, Jiang T, Liu Y-X, Bai YC, Reed J, Qu B, Goossens A, Nützmann H-W, Bai Y, Bai Y,
631 Osbourn A. 2019. A specialized metabolic network selectively modulates Arabidopsis root
632 microbiota. Science 364.

633 56. Ryan RP, Monchy S, Cardinale M, Taghavi S, Crossman L, Avison MB, Berg G, van der Lelie
634 D, Dow JM. 2009. The versatility and adaptation of bacteria from the genus
635 Stenotrophomonas. Nature Reviews Microbiology 7:514–525.

636 57. Erb M, Kliebenstein DJ. 2020. Plant Secondary Metabolites as Defenses, Regulators, and
637 Primary Metabolites: The Blurred Functional Trichotomy. Plant Physiology 184:39–52.

638 58. Wickham H, Averick M, Bryan J, Chang W, McGowan LD, François R, Grolemund G, Hayes A,
639 Henry L, Hester J, Max Kuhn, Kuhn M, Pedersen TL, Miller E, Bache SM, Müller K, Ooms J,
640 Robinson DG, Robinson D, David Robinson, Dana Seidel, Seidel DP, Spinu V, Takahashi K,
641 Kohske Takahashi, Vaughan D, Claus Wilke, Wilke CO, Woo KH, Yutani H. 2019. Welcome
642 to the Tidyverse. J Open Source Softw 4:1686.

643 59. Robinson D. 2014. broom: An R Package for Converting Statistical Analysis Objects Into
644 Tidy Data Frames. arXiv: Computation.

645 60. Wright ES. 2016. Using DECIPHER v2.0 to Analyze Big Biological Sequence Data in R. R
646 Journal 8:352–359.

647 61. Love MI, Huber W, Anders S. 2014. Moderated estimation of fold change and dispersion for
648 RNA-seq data with DESeq2. Genome Biology 15:550–550.

649 62. Lenth R, Sigmann H, Love J, Buerkner P, Herve M. 2019. emmeans: Estimated Marginal
650 Means, aka Least-Squares Means.

651 63. Arnold JB. 2019. Extra Themes, Scales and Geoms for “ggplot2” [R package ggthemes
652 version 4.2.4].

653 64. Kolde R. 2019. pheatmap: Pretty Heatmaps (1.0.12).

654 65. Hothorn T, Bretz F, Westfall PH. 2008. Simultaneous inference in general parametric
655 models. Biometrical Journal 50:346–363.

656 66. McMurdie PJ, Holmes S. 2013. phyloseq: an R package for reproducible interactive analysis
657 and graphics of microbiome census data. PLOS ONE 8.

658 67. Revell LJ. 2012. phytools: an R package for phylogenetic comparative biology (and other
659 things). Methods in Ecology and Evolution 3:217–223.

660 68. Oksanen J, Blanchet F, Friendly M, Kindt R, Legendre P, McGlinn D, Minchin P, O'Hara R,
661 Simpson G, Solymos P, Stevens M, Szoecs E, Wagner H. 2019. vegan: Community Ecology
662 Package.

663 69. Callahan BJ, McMurdie PJ, Rosen MJ, Han AW, Johnson AJA, Johnson A, Holmes S. 2016.
664 DADA2: High-resolution sample inference from Illumina amplicon data. Nature Methods
665 13:581–583.

666 70. Edgar RC. 2010. Search and clustering orders of magnitude faster than BLAST.
667 Bioinformatics 26:2460–2461.

668

669

670 # Figure legends

671 **Figure 1: SynCom design and metabolization of MBOA. A)** List of bacterial strains selected for
672 the non-metabolizing SynCom (nonSC) and the metabolizing SynCom (metSC) indicated with a
673 "+" if included and a "-" if not included. The phenotypes of each strain in MBOA metabolization
674 (Met, data from Ref 40) and MBOA tolerance (Tol, based on 2'500 µM data from Fig. S2) are listed
675 in columns three and four. (*) LMX9231 does not metabolize MBOA to AMPO in liquid culture, see
676 notes in Supplementary Results. **B)** The nonSC and metSC SynComs were grown in 96-well plates
677 containing 50% TSB supplemented with 500 µM MBOA for 68 h and afterwards the
678 metabolization of MBOA to AMPO and/or HMPAA was determined. SynComs and their no
679 bacteria controls (NBC, media with MBOA but without bacteria) were grown in triplicates and
680 pooled before measurements (n = 1).

681 **Figure 2: Metabolite profiles.** MBOA, AMPO and HMPAA were measured for dropout SynComs
682 (A) and paired cultures (B) after growth with MBOA. Heatmaps display the qualitative detections
683 of MBOA, AMPO and HMPAA. Detected compound levels were classified as "low" or "high" and are
684 indicated with light and dark color tones, respectively. Stacked bargraphs display the quantitative
685 metabolite measurements. SynComs and paired strains were grown in 96-well plates in liquid
686 50% TSB supplemented with 500 µM of MBOA alongside their no bacteria controls (NBC, media
687 with MBOA but without bacteria). Cultures were grown in triplicates and pooled before
688 measurements (n = 1).

689 **Figure 3: The metSC SynCom can use MBOA as sole carbon source.** The two SynComs were
690 grown in 96-well plates in minimal medium supplemented with 500 and 2'500 µM MBOA or
691 glucose (positive controls). Minimal medium supplemented with DMSO only was used as negative
692 control. Bacterial growth over 68 h is reported as the area under the growth curve (AUC) derived
693 from OD_{600} measurements over time. Means ± standard error and individual data points are
694 shown (n = 5). Asterisks indicate significant differences between treatment (pairwise t-test,
695 Bonferroni-adjusted $P < 0.05$).

696 **Figure 4: Size and composition of the nonSC and metSC SynComs in presence and absence**
697 **of MBOA.** SynComs were grown in shake flasks in 50% TSB supplemented with 500 µM or
698 2500 µM MBOA or DMSO only for 68 h. Five replicate cultures were set up for each SynCom and
699 treatment and two parallel samples of each culture were collected for community analysis by 16S
700 rRNA gene amplicon sequencing. **A)** Bacterial growth determined by OD_{600} at the end of the
701 experiment (n = 5). Asterisks indicate significant differences between the two SynComs (pairwise
702 t-test, Bonferroni-adjusted $P < 0.05$) **B** and **C)** Community compositions at the end of the
703 experiment. Shown are a Canonical analysis of Principal Coordinates (CAP) based on Bray-Curtis

704 distances and the model ~SynCom * treatment (n = 10) **(B)** and relative abundances of the
705 SynCom members for individual samples **(C)**.

706

707

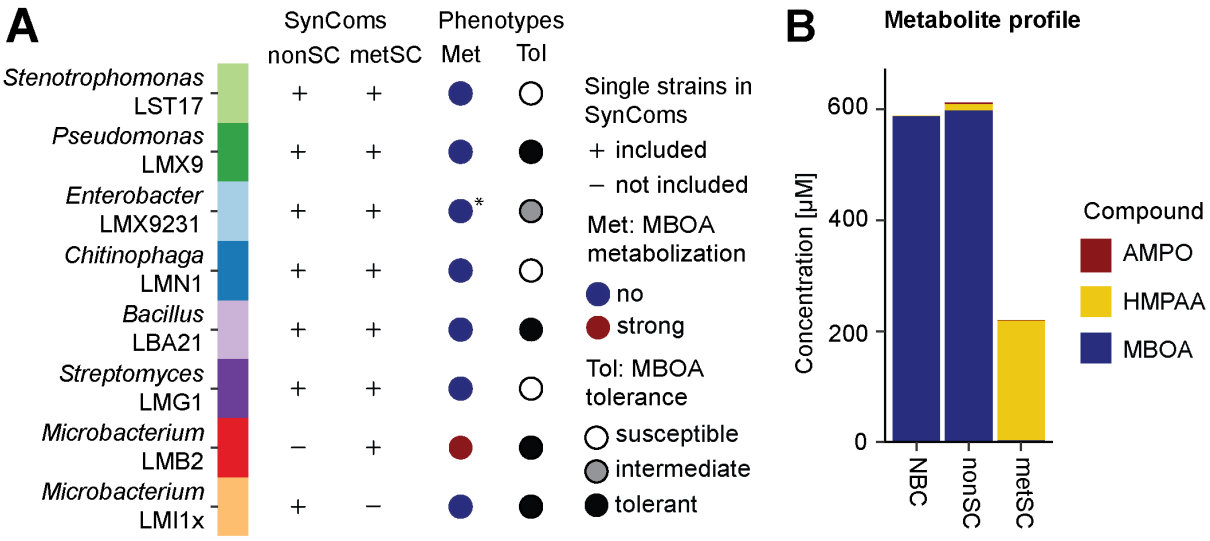

Figure 1: SynCom design and metabolisation of MBOA. A) List of bacterial strains selected for the non-metabolizing SynCom (nonSC) and the metabolizing SynCom (metSC) indicated with a "+" if included and a "-" if not included. The phenotypes of each strain in MBOA metabolization (Met, data from our previous publication (1)) and MBOA tolerance (Tol, based on 2'500 µM data from Fig. S2) are listed in columns three and four. (*) LMX9231 does not metabolize MBOA to AMPO in liquid culture, see notes in Supplementary Results. **B)** The nonSC and metSC SynComs were grown in 96-well plates containing 50% TSB supplemented with 500 µM MBOA for 68 h and afterwards the metabolisation of MBOA to AMPO and/or HMPAA was determined. SynComs and their no bacteria controls (NBC, media with MBOA but without bacteria) were grown in triplicates and pooled before measurements (n=1).

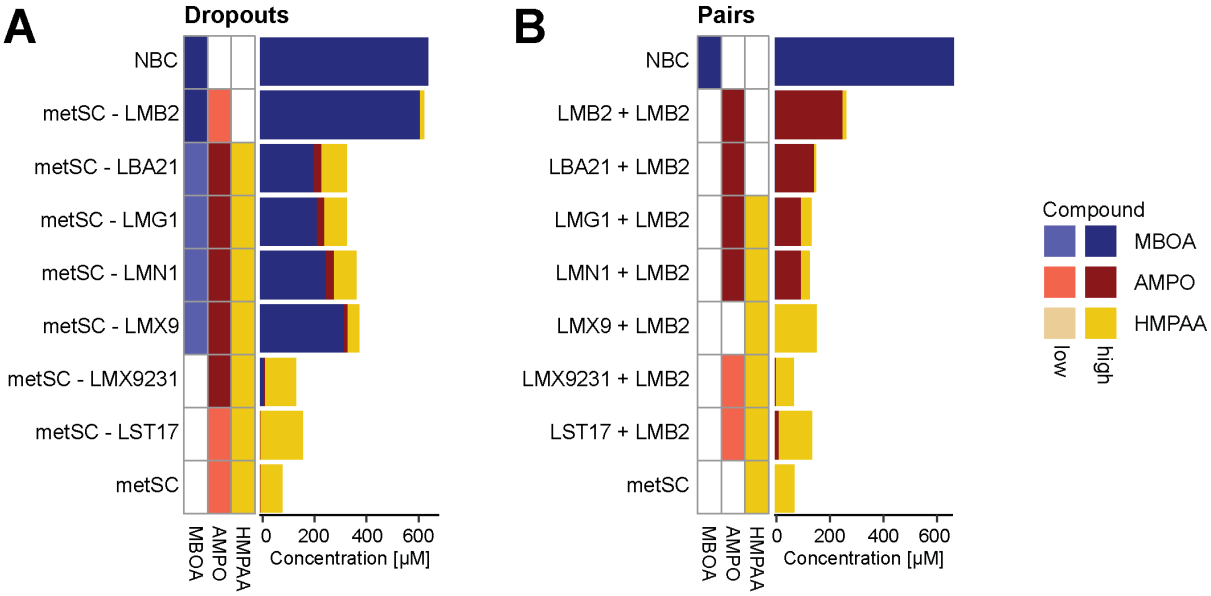

Figure 2: Metabolite profiles. MBOA, AMPO and HMPAA were measured for dropout SynComs (A) and paired cultures (B) after growth with MBOA. Heatmaps display the qualitative detections of MBOA, AMPO and HMPAA. Detected compound levels were classified as "low" or "high" and are indicated with light and dark color tones, respectively. Stacked bargraphs display the quantitative metabolite measurements. SynComs and paired strains were grown in 96-well plates in liquid 50% TSB supplemented with 500 µM of MBOA alongside their no bacteria controls (NBC, media with MBOA but without bacteria). Cultures were grown in triplicates and pooled before measurements (n = 1).

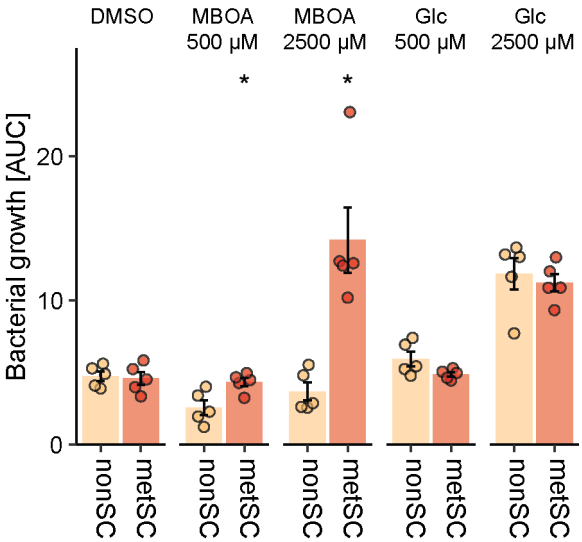

Figure 3: The metSC SynCom can use MBOA as sole carbon source. The two SynComs were grown in 96-well plates in minimal medium supplemented with 500 and 2'500 µM MBOA or glucose (positive controls). Minimal medium supplemented with DMSO only was used as negative control. Bacterial growth over 68 h is reported as the area under the growth curve (AUC) derived from OD_{600} measurements over time. Means ± standard error and individual data points are shown (n = 5). Asterisks indicate significant differences between treatment (pairwise t-test, Bonferroni-adjusted $P < 0.05$).

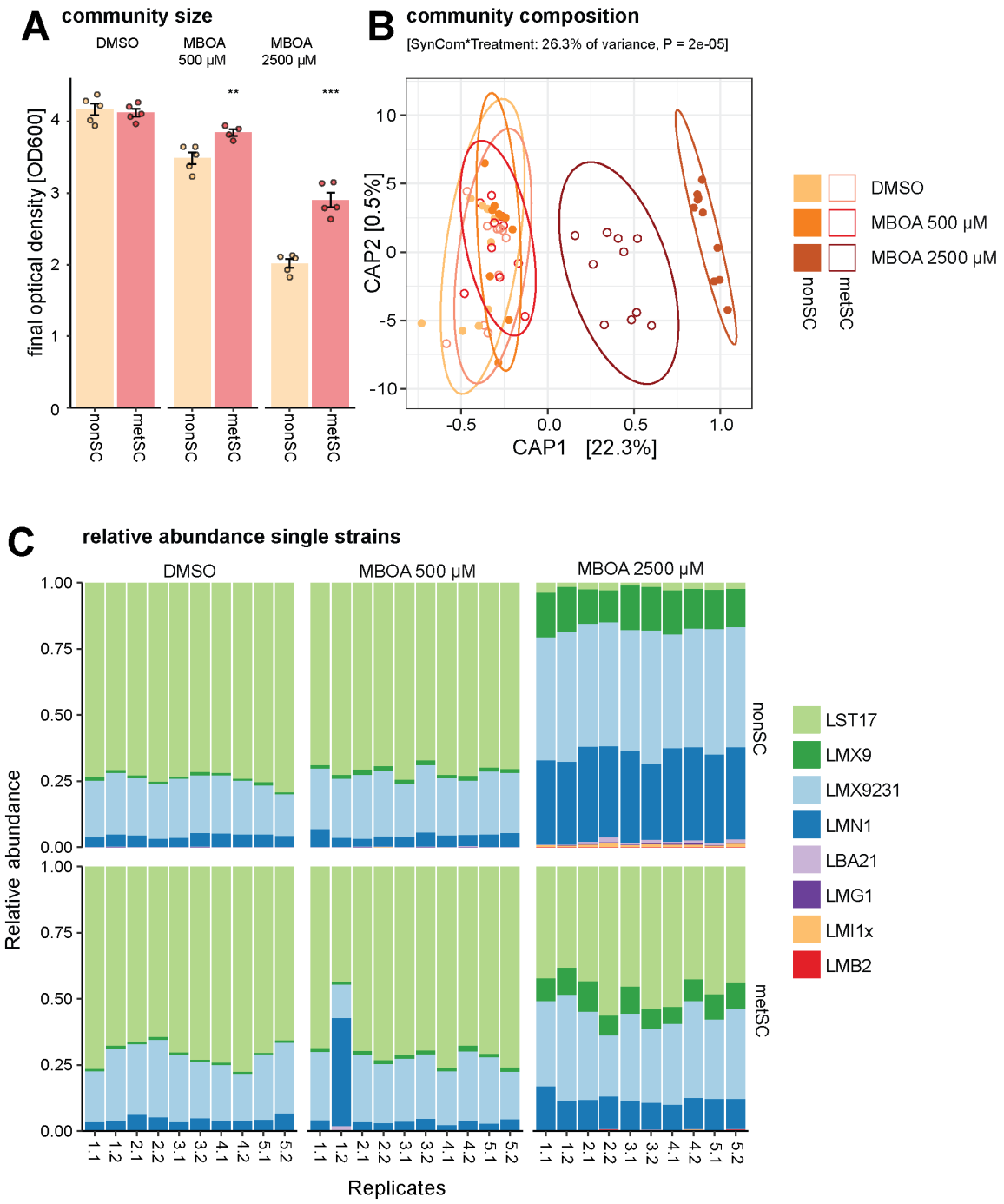

Figure 4: Size and composition of the nonSC and metSC SynComs in presence and absence of MBOA. SynComs were grown in shake flasks in 50% TSB supplemented with 500 µM or 2500 µM MBOA or DMSO only for 68 h. Five replicate cultures were set up for each SynCom and treatment and two parallel samples of each culture were collected for community analysis by 16S rRNA gene amplicon sequencing. **A)** Bacterial growth determined by OD_{600} at the end of the experiment (n = 5). Asterisks indicate significant differences between the two SynComs (pairwise t-test, Bonferroni-adjusted $P < 0.05$) **B** and **C)** Community compositions at the end of the experiment. Shown are a Canonical analysis of Principal Coordinates (CAP) based on Bray-Curtis distances and the model ~SynCom * treatment (n = 10) **(B)** and relative abundances of the SynCom members for individual samples **(C)**.

Supplementary Information

Synthetic communities of maize root bacteria interact and redirect benzoxazinoid metabolisation

Lisa Thoenen[1,2], Tobias Zuest[1,3], Christine Pestalozzi[2], Marco Kreuzer[4], Pierre Mateo[1], Gabriel Deslandes[1], Christelle A.M. Robert[1], Rémy Bruggmann[4], Matthias Erb[1], Klaus Schlaeppi[1,2 *]

[1] Institute of Plant Sciences, University of Bern, Bern, Switzerland
[2] Department of Environmental Sciences, University of Basel, Basel, Switzerland
[3] Department of Systematic and Evolutionary Botany, University of Zurich, Zurich, Switzerland
[4] Interfaculty Bioinformatics Unit, University of Bern, Bern, Switzerland
* Corresponding author: Klaus Schlaeppi, klaus.schlaeppi@unibas.ch

Running Head: "Benzoxazinoid metabolisation in synthetic communities" (49 ch.)

Index

- Supplementary Methods
- Supplementary Results
- Supplementary Figures
- Supplementary Tables
- Supplementary References

Supplementary Methods

Experiments

Experiment 1 (Figure 1A and S2): We cultured the nonSC and metSC SynComs in 96-well plates containing liquid 50% TSB supplemented with a final concentration of 500 µM MBOA. The experiment was stopped at 68 h. SynCom and NBC samples were grown in triplicates and pooled 1:1:1 for metabolite analysis. Fixing of bacterial cultures and metabolite analysis was performed as detailed below.

Experiment 2 (Figure 1B): We repeated Experiment 1 with the nonSC and metSC SynComs (liquid 50% TSB, 500 µM MBOA) but as a time-series to characterise the kinetics of MBOA degradation and AMPO or HMPAA formation. For metabolite sampling, we removed replicate plates from the stacker at 16, 24, 44, 68 and 96 h. SynCom and NBC samples were grown in triplicates and pooled 1:1:1 for metabolite analysis. Fixing of bacterial cultures and metabolite analysis was performed as detailed below.

Experiment 3 (Figure 2): We tested the nonSC and metSC SynComs, relative to single strain dropout SynComs (the metSC, minus the indicated strain) and each strain in paired cultures with *Microbacterium* LMB2. These assays were performed in liquid 50% TSB containing 500 µM MBOA and were stopped at 68 h. SynComs, the paired cultures and their non-bacterial controls (NBC, media with MBOA but without bacteria) were grown in triplicates and pooled 1:1:1 for metabolite analysis. Fixing of bacterial cultures and metabolite analysis was performed as detailed below. Classification of compound levels as "low" (>30% MBOA degraded compared to the NBC, <10% of max. AMPO-former (LMB2), <10% of max. HMPAA-former) or "high" (>90% MBOA degraded, >10% of max. AMPO-former (LMB2), >10% of max. HMPAA-former), were done as in our previous study (1).

Experiment 4 (Figure 3): In parallel with Experiment 1, we tested the single strains and both complete SynComs, each with 5 replicates, for whether they could use MBOA as sole carbon source for growth. We followed the same procedure as described above but used minimal media (described previously (2)) containing MBOA at concentrations of 500 and 2'500 µM. As positive controls for growth, we grew the bacteria in minimal medium supplemented with glucose (500 and 2'500 µM) as sole carbon source. We continuously recorded the OD_{600} of the cultures and stopped the experiment at 68 h. For a measure of bacterial growth, we calculated the area under the growth curve (AUC, x-axis for time and y-axis for OD_{600}) of the OD_{600} readings using the function *auc()* from package MESS (3) in R. We normalized growth in each treatment relative to the control. See analysis scripts for details.

Experiment 5 (Figure 4): For scale reasons, this experiment was performed in Erlenmeyer flasks and not in 96-well plates as the other experiments. Modifications include that the strains were pre-cultured overnight in 50 ml Erlenmeyer flasks containing 30 ml liquid 50% TSB and then mixed in equal ratios (OD_{600} = 0.6) as nonSC and metSC SynComs. The assembled SynComs were pelleted (5 min at 3'600 rpm), washed twice with 10 mM $MgCl_2$ buffer (Sigma-Aldrich, St. Louis, USA) and diluted in 35 mL of 10 mM $MgCl_2$. Samples of these 'input' SynComs (i.e. SynComs at the start of the experiment when inoculating the Erlenmeyer flasks) were aliquoted in 1.5 ml microcentrifuge tubes (5 replicates) and stored at -80 °C for community analysis. The same concentration of 10 mM $MgCl_2$ was added to the control treatment (NBC). Analogous to Experiments 1 – 4, cultures were grown in liquid 50% TSB supplemented with either 500 or 2'500 µM of MBOA or DMSO as a control. Five replicate cultures were set up for each of the 6 sample groups (2 SynCom * 3 treatments). The experiment was stopped at 68 h and the OD_{600} of each culture was recorded using a biophotometer (Eppendorf, Hamburg, Germany). Of each sample group, aliquots were fixed for metabolite analysis (details below). Metabolite measurements (n = 1) were made on pools of the five replicate cultures per sample group (pooled 1:1…). We also collected samples for community analysis by 16S rRNA gene amplicon sequencing (see below). For each of the 5 replicates per sample group, we collected two samples of the same culture resulting in n=10 replicates for community analysis. The samples were stored at -80 °C until processing. Finally, we assessed community size for each replicate (n=5) per sample group based on colony forming units (CFU) determined by plating serial dilutions on TSA plates and counting them at 22 °C.

Metabolite analysis from bacterial cultures

Samples for metabolite analyses were processed and measured as described previously (1). To fix the metabolites in the bacterial cultures, we added 150 µL of the cultures to 350 µL of extraction buffer (100% methanol (MeOH) + 0.14% formic acid (FA)) in non-sterile round bottom 96-well plates (Thermo Fisher Scientific, Waltham, USA). We stored the fixed samples with a final concentration of 70% MeOH and 0.1% FA at -80 °C. To reduce the number of samples, we pooled replicates of the same sample group. We diluted the pooled sample by adding 50 to 700 µL MeOH 70% + 0.1% FA and filtered the cultures through regenerated cellulose membrane filters (CHROMAFIL RC, 0,2 µm; Macherey-Nagel, Düren, Germany) by centrifugation (3'220 g for 2 min) to remove bacterial debris. To pellet any residual particles, we centrifuged the extracts at 11'000 g for 10 min at 4 °C. We aliquoted the supernatants in analytical glass vials (Screw Neck Vials, 1 ml; VWR, Dietikon, Switzerland) and stored the samples at -20 °C until analysis.

We profiled the benzoxazinoids and their degradation products in the fixed and filtered extracts of the bacterial cultures using an Acquity I-Class UHPLC system (Waters, Milford, US)

coupled to a Xevo G2-XS QTOF mass spectrometer (Waters, Milford, US) equipped with a LockSpray dual electrospray ion source (Waters, Milford, US). Gradient elution was performed on an Acquity BEH C18 column (2.1 x 100 mm i.d., 1.7 mm particle size; Waters, Milford, US) at 98–50% A over 6 min, 50-100% B over 2 min, holding at 100% B for 2 min, re-equilibrating at 98% A for 2 min, where A = water + 0.1% FA and B = acetonitrile + 0.1% FA. The flow rate was 0.4 mL/min. The temperature of the column was maintained at 40 °C, and the injection volume was 1 µL. The QTOF MS was operated in sensitivity mode with a positive polarity. The data were acquired over an m/z range of 50–1'200 with scans of 0.1 s at a collision energy of 6 V (low energy) and a collision energy ramp from 10 to 30 V (high energy). The capillary and cone voltages were set to 2 kV and 20 V, respectively. The source temperature was maintained at 140°C, the desolvation temperature was 400 °C at 1'000 L/hr and the cone gas flow was 100 L/hr. Accurate mass measurements (<2 ppm) were obtained by infusing a solution of leucine encephalin at 200 ng/mL at a flow rate of 10 µL/min through the Lockspray probe (Waters, Milford, US). For each expected benzoxazinoid, standard compounds with four concentrations were run together with the samples (DIMBOA-Glc, DIMBOA, HMBOA, MBOA-Glc, MBOA, BOA, AMPO, APO, AAMPO, HMPMA, each at 10, 50, 200, and 400 ng/mL; HMPAA at 40, 200 ng/mL, 1 and 10 µg/mL). Here in this work, we only report MBOA, AMPO and HMPAA. The compound peaks in the raw chromatogram data were integrated using MassLynx 4.1 (Waters, Milford, US) and identified based on the reference compounds in the standards. Further, we searched for candidate compounds increasing in metSC over time using Progenesis QI Software (Waters, Milford, USA) and analysed it in R statistical software. All source data and R code used for graphing are available from https://github.com/PMI-Basel/Thoenen_et_al_SynCom.

DNA extraction, library prep and sequencing

The DNA was extracted from two technical replicates per culture using the NucleoSpin Soil kit (Macherey-Nagel, Düren, Germany). For DNA extraction, 1 ml of culture was pelleted at 13'000 rpm, then the first buffer was directly added to the pellet. Afterwards the extraction was performed following the manufacturer's instructions. The DNA concentration was quantified with the AccuClear® Ultra High Sensitivity dsDNA Quantitation Kit (Biotium, Fremont, USA). DNA was diluted to 0.2 ng/µl for subsequent amplification. A two-step PCR was performed, where with first PCR the DNA is amplified and in the second PCR the PCR products are tagged with custom barcodes. For the first PCR, the 16s rRNA gene was amplified with the specific primers 515-F (GTGYCAGCMGCCGCGGTAA, (4) and 806*-R (TTAGAWACCCBNGTAGTCC). The 806*-R was shortened by one base to avoid mismatch with the 16S sequence of the microbacteria strains. The PCR reaction mix was composed of 5 µl DNA template, 0.4 µl of 10 µM 515-F and 806*-R primers each, 8 µl 5Prime HotMasterMix (Quantabio, Beverly, USA), 2 µl 3% BSA and 4.6 µl autoclaved

MilliQ water to a final reaction volume of 20 µl. The cycling profile was 94°C for 3 minutes, 25 cycles of 94°C for 45 seconds, 60°C for 60 seconds, 72°C for 90 seconds, and 72°C for ten minutes. All PCR reactions were purified with SPRIselect beads (Beckman Coulter Life Sciences, Indianapolis, USA) following manufacturer's instructions. The reaction products from the first PCR were next amplified for another 10 cycles with uniquely barcoded primer pairs for each sample in a second PCR. The barcoded PCR products were purified with SPRIselect beads, DNA was quantified with the Qubit™ dsDNA BR kit (Invitrogen, Thermo Fisher Scientific, Waltham, MA, USA), and the samples were pooled equimolar using a Myra Liquid Handler (Bio Molecular Systems, Upper Coomera, Australia). The pooled library was bead purified and sequenced by MiSeq v2 500 cycle nano sequencing kit at the Next Generation Sequencing Platform (University of Bern) using the 2x 250 bp pair-end sequencing protocol (Illumina Inc., San Diego, USA).

Community analysis details

The raw sequencing data was processed in R using the DADA2 pipeline version 1.20 (70). The analysis steps were wrapped in a Snakemake pipeline (5). In brief, raw reads were filtered and trimmed with the function *filterAndTrim()*. This step trims the 19 bp long primer sequences (trimLeft and trimRight = 19) and discards low-quality reads (truncQ = 2), reads matching PhiX and reads containing Ns. The reads were then subjected to the error learning step using *learnErrors()*, dereplicated using *derepFastq()* and denoised using dada(derepFs, err=errF, multithread=TRUE) following the DADA2 pipeline with default options. Next, the read pairs were merged using *mergePairs()* (minimal overlap of 20 bp) and chimera were removed using *removeBimeraDenovo()*. Finally, taxonomic assignment of the high-quality sequences was done against the SILVA database (v128; (6) using *assignTaxonomy()* and *addSpecies()* functions. A phyloseq object was exported for downstream analysis. **Dataset S2** documents all the dada2 pipeline. The source code for the analysis of the raw sequencing data is available from https://github.com/makrez/Analysis_documentation_Synthetic_communities_mrb.

For analysis of the community data, we first mapped the 16S rRNA gene sequences of the the SynCom members (all MRB strains have Sanger sequences available; (7) to the amplicon sequences using usearch (8) with an identity of 0.97. ASVs mapping to the SynCom members were used for calculation, other low abundant and non-mapping ASVs were discarded. The counts of the community data were normalized by rarefaction using phyloseq (9) and the abundances of the strains were further adjusted based on their estimated copy numbers of the 16S rRNA genes (**Dataset S1**). Compositional differences between the SynComs and by the treatments were tested with Permutational Analysis of Variance (PERMANOVA, 99999 permutations; model: ~ SynCom * Treatment) on Bray Curtis distances using the R package vegan (10). The effects on community composition using the same model were visualized with a Canonical Analysis of Principal

coordinates (CAP) using the R package phyloseq (9). All source data and code used for statistical analysis and graphing are available from https://github.com/PMI-Basel/Thoenen_et_al_SynCom.

Supplementary Results

Phenotype of *Enterobacter* LMX9231

One of the six core bacteria of both SynComs, *Enterobacter* LMX9231, had been identified earlier to colour MBOA-containing agar red, indicating AMPO formation (**Fig. S2A**, 1). Evaluating this strain in liquid culture, we found that, even though the strain forms AMPO on plates, it does not degrade MBOA to AMPO in the liquid growth condition (**Fig. S2B**). This finding for liquid media was full consistent with all experiments of this study where the non-metabolising SynCom, of which LMX9231 is an abundant member (**Fig. 4C**), never degraded MBOA (see results of Experiments 1, 2 and 5). It appears plausible that *Enterobacter* LMX9231 may possess an alternative pathway for AMPO formation than Microbacteria and *Sphingobium*. When we found BxdA as an enzyme for the MBOA-to-AMPO metabolisation, we noticed that the best homologies to BxdA in *Enterobacteriaceae* showed less than 30% similarity on amino acid level. This low level of protein similarity was consistent with all tested strains that could not form AMPO-formation in liquid culture (**Fig. S2C**). We therefore think, that *Enterobacteriaceae* may possess another, BxdA-independent mechanism responsible for the AMPO-formation and this pathway seems to operate on Agar-plates and not in liquid cultures.

Supplementary Figures

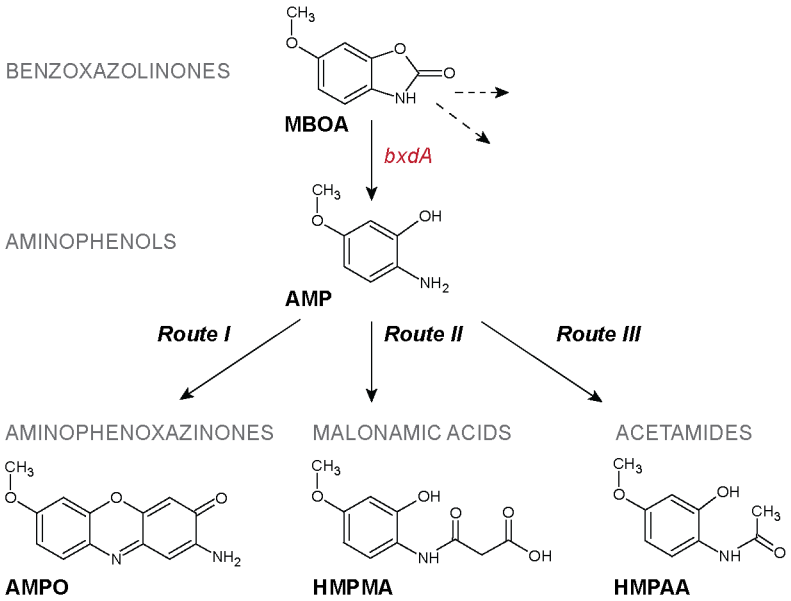

Abbreviation	Full name	Class	Mass [g/mol]	Formula
DIMBOA-Glc	2-O-β-D-glucopyranosyl-2,4-dihydroxy-7-methoxy-(2H)-1,4-benzoxazin-3(4H)-one	Benzoxazinone glucoside	373.31	C15H19NO10
DIMBOA	2,4-dihydroxy-7-methoxy-1,4-benzoxazin-3-one	Benzoxazinone aglucone	211.17	C9H9NO5
MBOA	6-methoxybenzoxazolin-2(3H)-one	Benzoxazolinone	165.15	C8H7NO3
BOA	Benzoxazolin-2-(3H)-one	Benzoxazolinone	135.10	C7H5NO2
AMP	2-amino-5-methoxyphenol	Aminophenol	139.15	C7H9NO2
AP	2-aminophenol	Aminophenol	109.13	C6H7NO
AAP	2-acetamidophenol	Acetamide	151.16	C8H9NO2
HMPAA	N-(2-hydroxy-4-methoxyphenyl)acetamide	Acetamide	181.19	C9H11NO3
HMPMA	N-(2-hydroxy-4methoxyphenyl)malonamic acid	Malonamic acid	225.2	C10H11NO5
AMPO	2-amino-7-methoxy-phenoxazin-3-one	Aminophenoxazinones	242.23	C13H10N2O3
APO	2-amino-(3H)-phenoxazin-3-one	Aminophenoxazinones	212.20	C12H8N2O2
AAMPO	2-acetylamino-7-methoxy-phenoxazin-3-one	Aminophenoxazinones	284.27	C15H12N2O4
AAPO	2-acetylamino-(3H)-phenoxazin-3-one	Aminophenoxazinones	254.24	C14H10N2O3

Supplementary Figure S1: Benzoxazinoid metabolites produced by plants and degradation pathways in soil. The table lists the full chemical name, the compound class, the molar mass and the chemical formula.

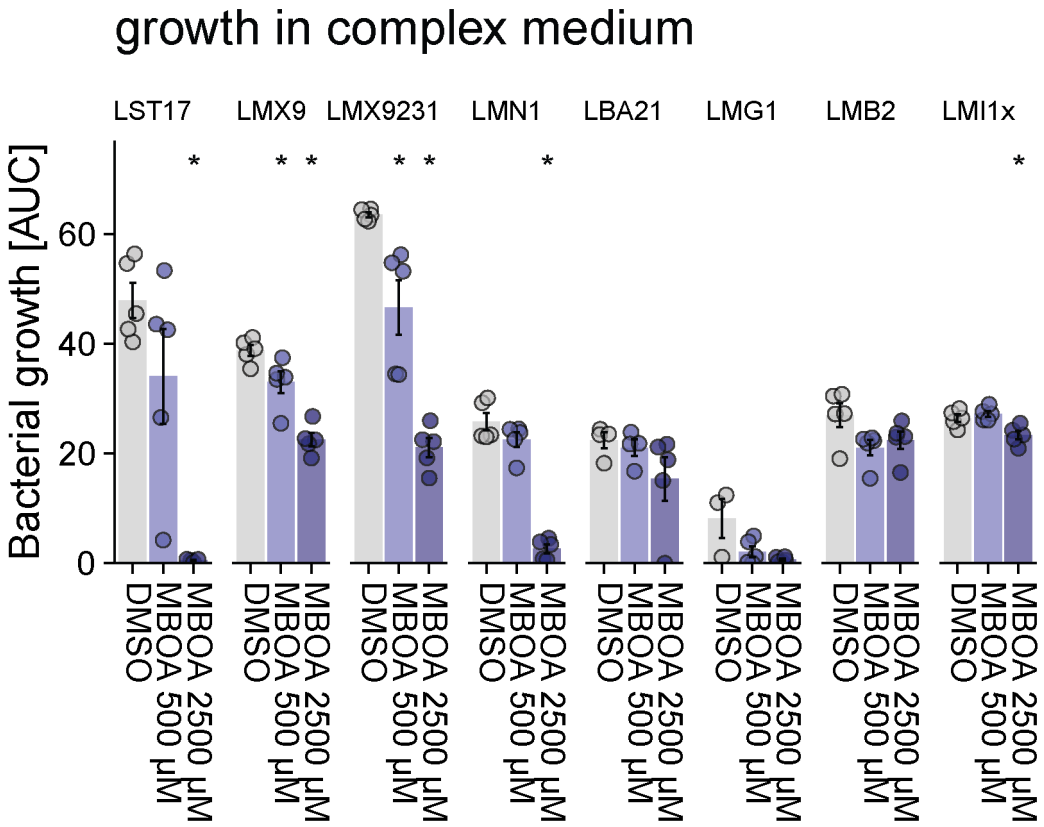

Supplementary Figure S2: Growth of individual SynCom members in presence of MBOA. Bacterial growth was assessed in 50% TSB supplemented with MBOA (500 and 2'500 µM) or DMSO only (negative control). Five replicates were grown for each strain (n = 5). Means ± standard errors are reported and asterisks indicate significant differences between treatments and DMSO controls (pairwise t-test, Bonferroni-adjusted $P < 0.05$).

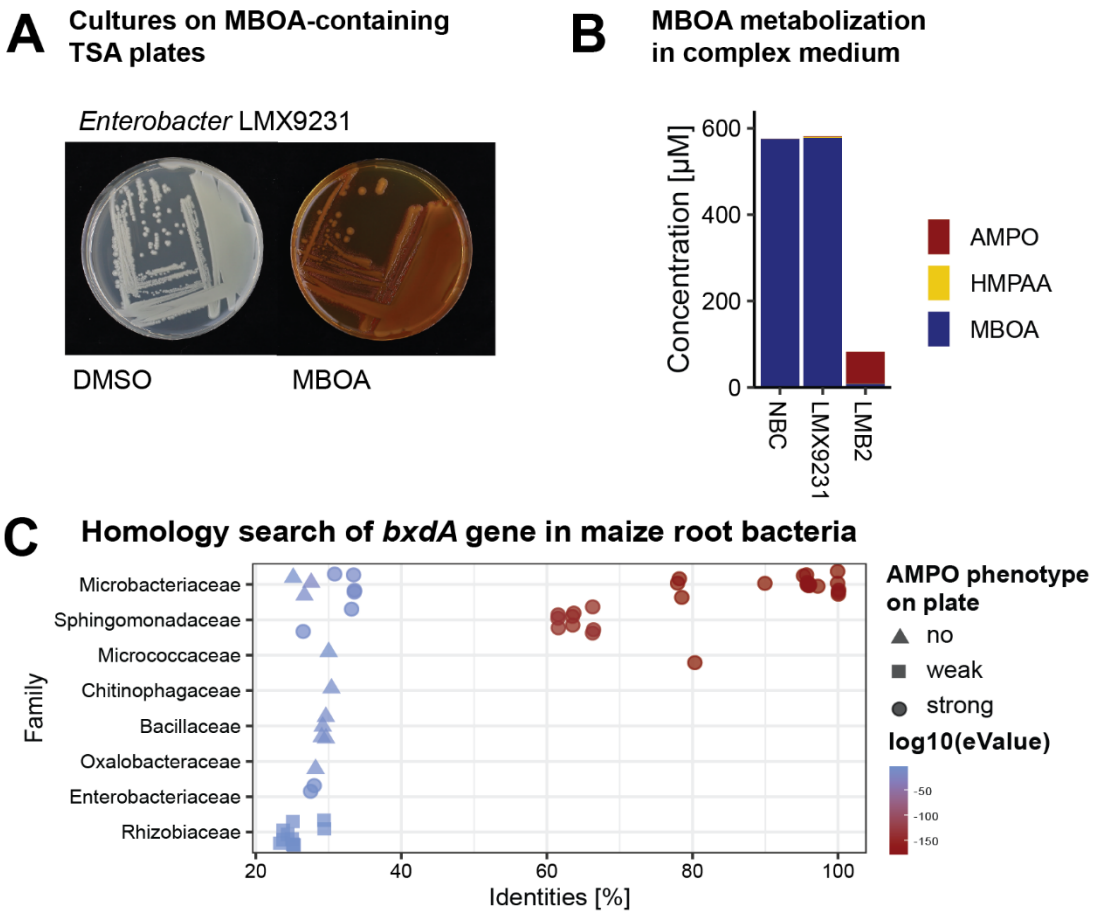

Supplementary Figure S2: MBOA metabolisation phenotype of *Enterobacter* LMX9231: A) Pictures of *Enterobacter* LMX9231 grown on 100% TSA plates containing DMSO (2 mL/L) or MBOA (200 mg/L; ~1'200 µM) for 10 days suggest AMPO formation. **B)** Metabolisation of MBOA and benzoxazinoid metabolites formed by *Enterobacter* LMX9231 and *Microbacterium* LMB2 (positive control) in 50% TSB supplemented with 500 µM MBOA show absence of MBOA metabolisation in liquid culture. **C)** Homology searches with the protein BxdA from *Microbacterium* LMB2 across all genome sequenced strains of the MRB collection. The panel C of this figure was shown in a previous publication (1).

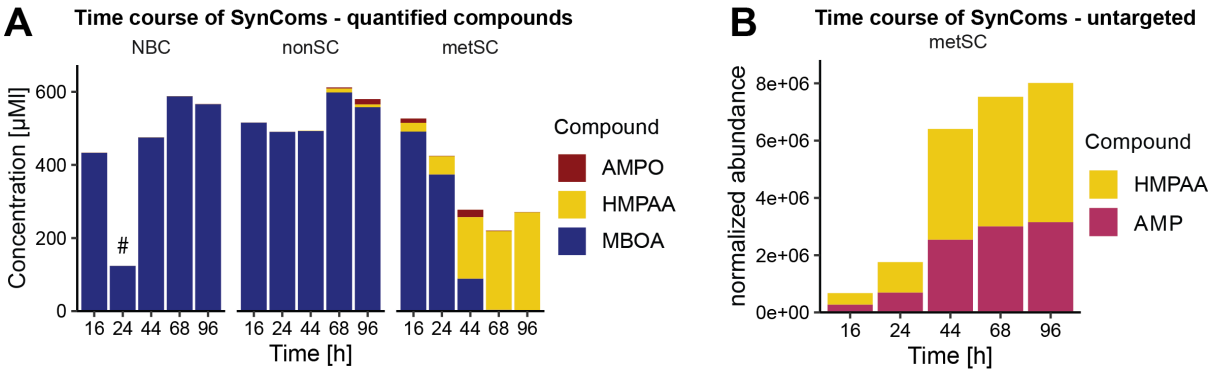

Supplementary Figure S3: Metabolisation of MBOA by SynComs. The nonSC and metSC SynComs were grown in 96-well plates containing 50% TSB supplemented with 500 µM MBOA and samples were collected at the indicated time points up to 96 h. The 68 h time point is shown in Fig. 1B. **A)** The concentrations of MBOA, AMPO and HMPAA metabolites were quantified using analytical standards while in **B)** the intermediate AMP (see Fig. S1) is reported based on the normalized peak area (peak corresponding to the mass of AMP). HMPAA is reported again but on its normalized peak area for reference. Metabolite measurements (n = 1) were made on pools of three independently grown cultures (#: sample with failed pooling). Part of panel A of this figure (NBC) was shown in a previous publication (1).

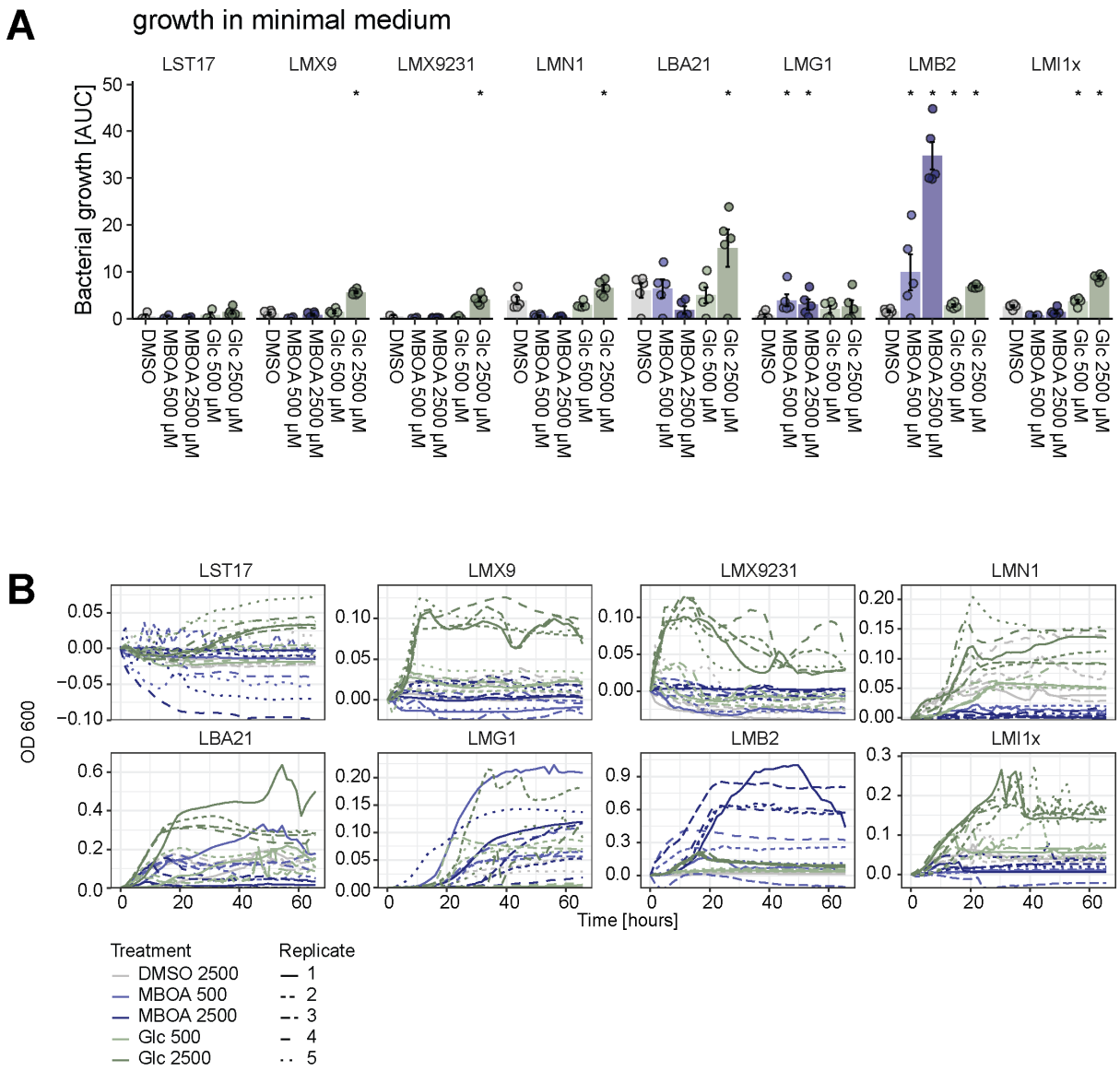

Supplementary Figure S4: Growth of individual SynCom members in minimal media. Bacterial growth in the minimal medium with DMSO (negative control), MBOA (500 and 2'500 µM) or glucose (positive control; same concentrations) as sole carbon sources. Five replicates were grown for each strain (n=5). Means ± standard errors are reported and asterisks indicate significant differences against their DMSO control (pairwise t-test, Bonferroni-adjusted $P < 0.05$). Part of the data of this figure was shown in a previous publication (1).

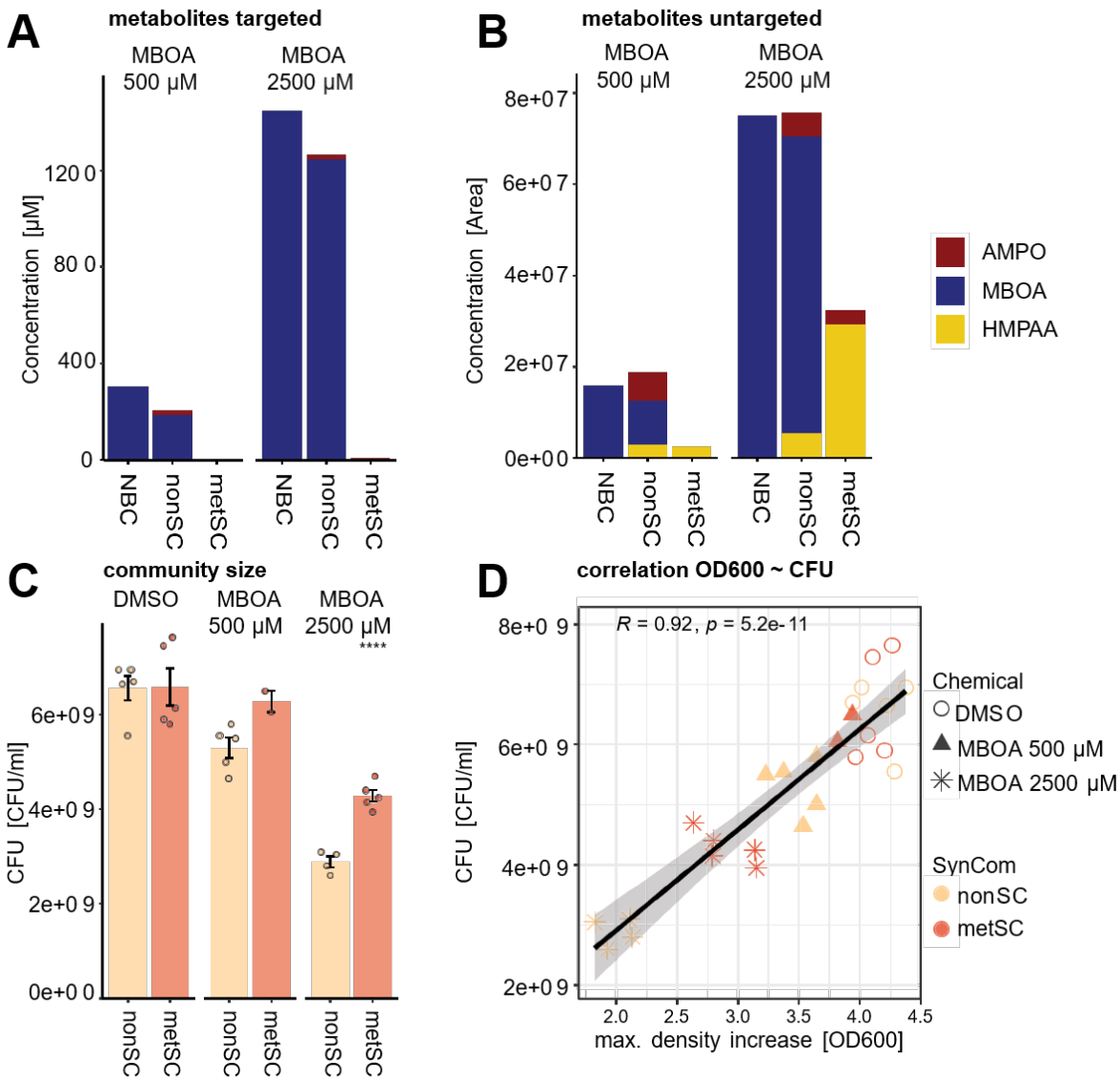

Supplementary Figure S5: Metabolites and growth of the SynComs in presence and absence of MBOA. SynComs were grown in shake flasks containing 20 mL 50% TSB supplemented with DMSO or 500 µM or 2'500 µM MBOA until harvest at 68 h. Five replicate cultures were set up for each SynCom and treatment. **A)** Measurements of metabolites after exposure of both SynComs and their no bacteria control (NBC, media with MBOA but without bacteria) to MBOA. Metabolite measurements (n = 1) were made on pools of five replicate cultures. Note that HMPAA is not shown in A because of absence of a standard. **B)** Untargeted measurements of metabolites, relative concentrations were calculated from the area of the integrated peaks. **C)** Community size was determined by counting the colony forming units (CFU/mL) at the end of the experiment (n=5). Asterisks indicate significant differences between the SynComs (pairwise t-test, Bonferroni-adjusted P < 0.05). **D)** Corrleation of the two measurements for bacterial growth, OD_{600} compared to CFU counts (shown in Fig. 4A).

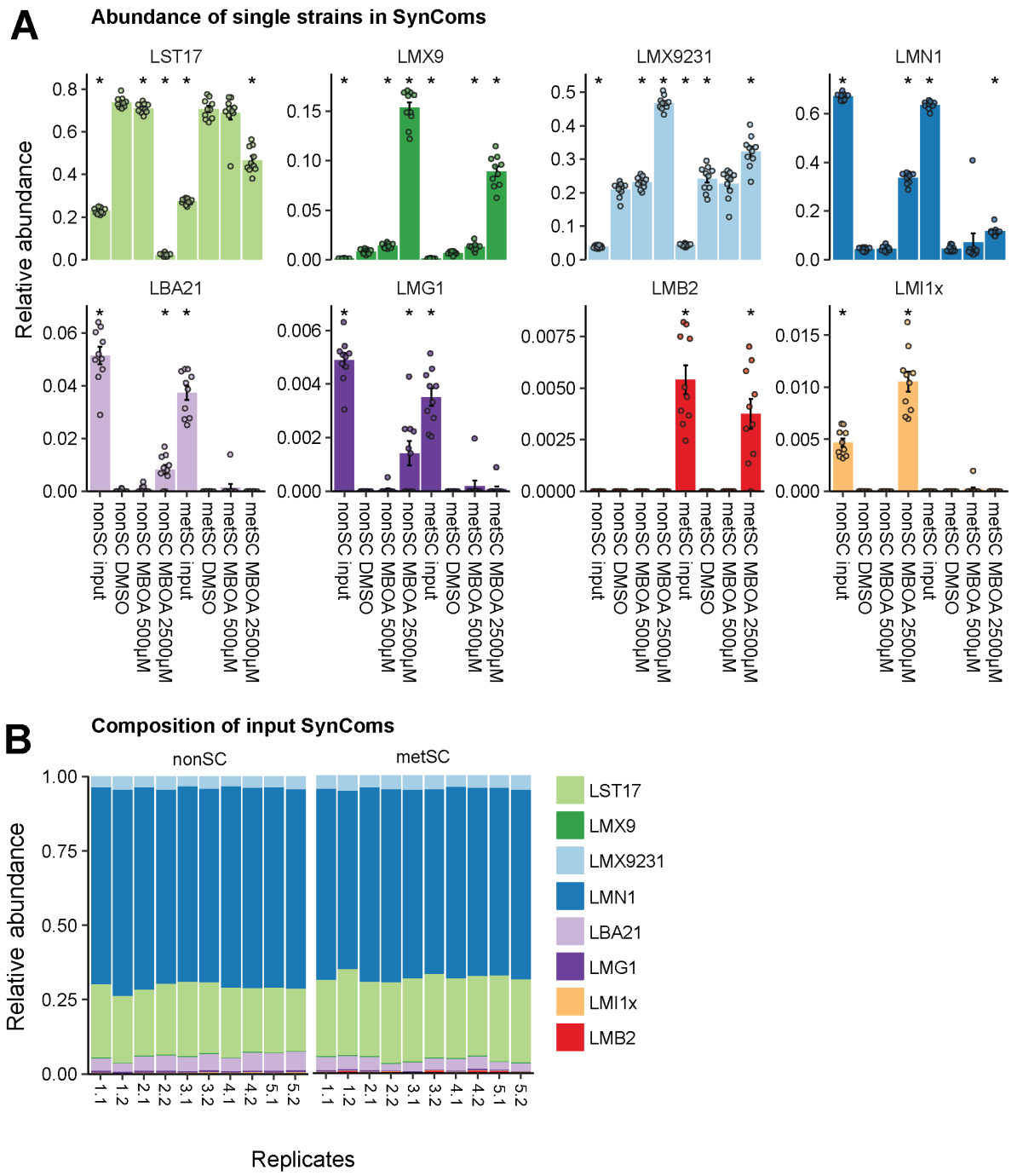

Supplementary Figure 6: Abundance of single strains in the SynComs in presence and absence of MBOA. SynComs were grown in shake flasks containing 20 mL 50% TSB supplemented with DMSO or 500 µM or 2500 µM MBOA until harvest at 68 h. Five replicate cultures were set up for each SynCom and treatment and two parallel samples of the same culture were collected for community analysis by 16S rRNA gene amplicon sequencing. **A)** Relative abundances of each single strain in the SynCom at the beginning of the experiment (input) and treatment combinations during the experiment. Asterisks indicate significant differences between the treatments (pairwise t-test, Bonferroni-adjusted $P < 0.05$). **B)** Community analysis was also conducted with the 'input' SynComs, i.e. to determine the strain abundances at the start of the experiment.

Supplementary Tables

Table S1: PERMANOVA of SynCom composition

Factorial effects on community compositions were assessed using PERMANOVA based on Bray Curtis distances and the model ~SynCom * Treatment (n=10).

	Df	SumOfSqs	R2	F	Pr(>F)
Treatment	2	0.7837848	0.2598361	10.467239	**0.001**
SynCom	1	0.0504273	0.0167174	1.346886	0.26
Treatment:SynCom	2	0.1604922	0.0532055	2.14333	0.063
Residual	54	2.0217547	0.6702411	NA	NA
Total	59	3.0164589	1	NA	NA

Supplementary Datasets

Dataset S1: Documentation of dada2 pipeline script used. This file is a html markdown of the R script containing the code to process the raw sequencing reads from the community profiling (Experiment 5) to the phyloseq object which was then further analysed in R.

Dataset S2: Table contains information on all bacterial strains used in the SynCom, taxonomy information, 16S sanger sequence and the number of 16S copies.

References

1. Thoenen L, Kreuzer M, Pestalozzi C, Florean M, Mateo P, Züst T, et al. The lactonase BxdA mediates metabolic specialisation of maize root bacteria to benzoxazinoids. Nat Commun. 2024 Aug 2;15(1):6535.

2. Peyraud R, Kiefer P, Christen P, Massou S, Portais JC, Vorholt JA. Demonstration of the ethylmalonyl-CoA pathway by using 13C metabolomics. Proc Natl Acad Sci U S A. 2009 Mar 24;106(12):4846–51.

3. Ekstrøm C. MESS: Miscellaneous Esoteric Statistical Scripts. 2016.

4. Ul-Hasan S, Bowers RM, Figueroa-Montiel A, Licea A, Licea-Navarro AF, Beman JM, et al. Community ecology across bacteria, archaea and microbial eukaryotes in the sediment and seawater of coastal Puerto Nuevo, Baja California. PLOS ONE. 2019 Feb 14;14(2).

5. Mölder F, Jablonski KP, Letcher B, Hall MB, Tomkins-Tinch CH, Sochat V, et al. Sustainable data analysis with Snakemake. F1000Research. 2021;10:33.

6. Callahan B. Silva Taxonomic Training Data Formatted For Dada2 (Silva Version 128). 2017 Jan 1;

7. Thoenen L, Giroud C, Kreuzer M, Waelchli J, Gfeller V, Deslandes-Hérold G, et al. Bacterial tolerance to host-exuded specialized metabolites structures the maize root microbiome. Proc Natl Acad Sci. 2023 Oct 31;120(44):e2310134120.

8. Edgar RC. Search and clustering orders of magnitude faster than BLAST. Bioinformatics. 2010 Oct 1;26(19):2460–1.

9. McMurdie PJ, Holmes S. phyloseq: an R package for reproducible interactive analysis and graphics of microbiome census data. PLOS ONE. 2013 Apr 22;8(4).

10. Oksanen J, Blanchet F, Friendly M, Kindt R, Legendre P, McGlinn D, et al. vegan: Community Ecology Package. 2019.